

From trace to trace maker: Oligocene-Miocene coprolites of southern Poland and their potential producers (#118793)

1

First submission

Guidance from your Editor

Please submit by **2 Jun 2025** for the benefit of the authors (and your token reward) .



Structure and Criteria

Please read the 'Structure and Criteria' page for guidance.



Raw data check

Review the raw data.



Image check

Check that figures and images have not been inappropriately manipulated.

All review materials are strictly confidential. Uploading the manuscript to third-party tools such as Large Language Models is not allowed.

If this article is published your review will be made public. You can choose whether to sign your review. If uploading a PDF please remove any identifiable information (if you want to remain anonymous).

Files

Download and review all files from the [materials page](#).

13 Figure file(s)

4 Table file(s)

1 Video file(s)




Structure and Criteria

Structure your review

The review form is divided into 5 sections. Please consider these when composing your review:

1. BASIC REPORTING
2. EXPERIMENTAL DESIGN
3. VALIDITY OF THE FINDINGS
4. General comments
5. Confidential notes to the editor






 You can also annotate this PDF and upload it as part of your review

When ready [submit online](#).





Editorial Criteria

Use these criteria points to structure your review. The full detailed editorial criteria is on your [guidance page](#).




BASIC REPORTING

-  Clear, unambiguous, professional English language used throughout.
-  Intro & background to show context. Literature well referenced & relevant.
-  Structure conforms to [Peerj standards](#), discipline norm, or improved for clarity.
-  Figures are relevant, high quality, well labelled & described.
-  Raw data supplied (see [Peerj policy](#)).

EXPERIMENTAL DESIGN

-  Original primary research within [Scope of the journal](#).
-  Research question well defined, relevant & meaningful. It is stated how the research fills an identified knowledge gap.
-  Rigorous investigation performed to a high technical & ethical standard.
-  Methods described with sufficient detail & information to replicate.

VALIDITY OF THE FINDINGS

-  **Impact and novelty is not assessed.** Meaningful replication encouraged where rationale & benefit to literature is clearly stated.
-  All underlying data have been provided; they are robust, statistically sound, & controlled.
-  Conclusions are well stated, linked to original research question & limited to supporting results.



The best reviewers use these techniques

Tip

Example

Support criticisms with evidence from the text or from other sources

Smith et al (J of Methodology, 2005, V3, pp 123) have shown that the analysis you use in Lines 241-250 is not the most appropriate for this situation. Please explain why you used this method.

Give specific suggestions on how to improve the manuscript

Your introduction needs more detail. I suggest that you improve the description at lines 57- 86 to provide more justification for your study (specifically, you should expand upon the knowledge gap being filled).

Comment on language and grammar issues

The English language should be improved to ensure that an international audience can clearly understand your text. Some examples where the language could be improved include lines 23, 77, 121, 128 - the current phrasing makes comprehension difficult. I suggest you have a colleague who is proficient in English and familiar with the subject matter review your manuscript, or contact a professional editing service.

Organize by importance of the issues, and number your points

1. Your most important issue
2. The next most important item
3. ...
4. The least important points

Please provide constructive criticism, and avoid personal opinions

I thank you for providing the raw data, however your supplemental files need more descriptive metadata identifiers to be useful to future readers. Although your results are compelling, the data analysis should be improved in the following ways: AA, BB, CC

Comment on strengths (as well as weaknesses) of the manuscript

I commend the authors for their extensive data set, compiled over many years of detailed fieldwork. In addition, the manuscript is clearly written in professional, unambiguous language. If there is a weakness, it is in the statistical analysis (as I have noted above) which should be improved upon before Acceptance.

From trace to trace maker: Oligocene-Miocene coprolites of southern Poland and their potential producers

Tomasz Brachaniec ^{Corresp., 1}, Dorota Środek ¹, Mateusz Salamon ¹, Michał Bugajski ², Piotr Duda ³, Adam Danielak ⁴, Magdalena Janiszewska ⁴, Grzegorz Sadlok ¹, Wojciech Kuśnierczyk ²

¹ Department of Natural Sciences, University of Silesia, Sosnowiec, Poland

² Fossil Amateur Club "Inkluzja", Łódź, Poland

³ Faculty of Science and Technology, University of Silesia, Sosnowiec, Poland

⁴ Municipal Zoological Garden in Łódź, Łódź, Poland

Corresponding Author: Tomasz Brachaniec
Email address: tomasz.brachaniec@us.edu.pl

In this paper we describe coprolites from deep-marine Oligocene sediments, shallow- and deep-marine Miocene deposits, as well as Miocene continental environments in southern and central Poland. The Oligocene coprolites are classified into five morphotypes: (1) sinusoidal, (2) straight to moderately curved, (3) regular forms with macroscopically visible vertebrate remains, (4) S-shaped, and (5) oval. Sinusoidal coprolites, previously interpreted as originating from predatory fish (e.g., *Palimphytes*, *Oligophus*, and indeterminate taxa), are reinterpreted here, based on actualistic observations, as crustacean (crab) feces. Morphotypes (2)–(4) are attributed to fish, while the oval type (5) is tentatively linked to columbid-like birds, although alternative producers cannot be excluded. Miocene deep-sea coprolites are represented by relatively long, complex fecal masses composed of constricted strings, suggesting holothurians or cephalopods as potential producers. Elongated Miocene coprolites from shallow-water environments are likely to have been produced by teleost fish - most likely Sparidae - or by sharks. However, other vertebrates, including toothed and toothless cetaceans and porpoises, cannot be ruled out. The terrestrial Miocene specimens include ferruginous masses with excrement-like morphologies, which, despite some controversy, are interpreted as coprolites likely produced by snakes. Another coprolite group comprises phosphatic, elongated specimens with a prominent pointed end, likely formed during anal contraction at the end of defecation. These are attributed to small mammals such as Sciuridae and/or Chiropteridae. Overall, these data provide new insights into the diversity of post-Mesozoic coprolites and refine our understanding of their producers and associated ecosystems in Central Europe.

1 **From Trace to Trace Maker: Oligocene–Miocene Coprolites**
2 **of Southern Poland and Their Potential Producers**

3

4 **Tomasz Brachaniec^{1*}, Dorota Środek¹, Mateusz Salamon¹, Michał Bugajski², Piotr Duda³,**
5 **Adam Danielak⁴, Magdalena Janiszewska⁴, Grzegorz Sadlok¹, Wojciech Kuśnierczyk²**

6

7 ¹University of Silesia in Katowice, Faculty of Natural Sciences, Sosnowiec, Poland

8 ²Fossil Amateur Club “Inkluzja”, Łódź, Poland

9 ³University of Silesia in Katowice, Faculty of Science and Technology, Sosnowiec, Poland

10 ⁴Municipal Zoological Garden in Łódź [Polish limited liability company], Łódź, Poland

11

12 *corresponding author – tomasz.brachaniec@us.edu.pl

13

14

15

16

17

18

19

20

21

22

23

24

25

26

27

28

29

30

31

32

33

34

35

36

37

38 **Abstract**

39

40 In this paper we describe coprolites from deep-marine Oligocene sediments, shallow- and deep-
41 marine Miocene deposits, as well as Miocene continental environments in southern and central
42 Poland. The Oligocene coprolites are classified into five morphotypes: (1) sinusoidal, (2) straight
43 to moderately curved, (3) regular forms with macroscopically visible vertebrate remains, (4) S-
44 shaped, and (5) oval. Sinusoidal coprolites, previously interpreted as originating from predatory
45 fish (e.g., *Palimphyes*, *Oligophus*, and indeterminate taxa), are reinterpreted here, based on
46 actualistic observations, as crustacean (crab) feces. Morphotypes (2)–(4) are attributed to fish,
47 while the oval type (5) is tentatively linked to columbid-like birds, although alternative producers
48 cannot be excluded. Miocene deep-sea coprolites are represented by relatively long, complex
49 fecal masses composed of constricted strings, suggesting holothurians or cephalopods as
50 potential producers. Elongated Miocene coprolites from shallow-water environments are likely
51 to have been produced by teleost fish - most likely Sparidae - or by sharks. However, other
52 vertebrates, including toothed and toothless cetaceans and porpoises, cannot be ruled out. The
53 terrestrial Miocene specimens include ferruginous masses with excrement-like morphologies,
54 which, despite some controversy, are interpreted as coprolites likely produced by snakes.
55 Another coprolite group comprises phosphatic, elongated specimens with a prominent pointed
56 end, likely formed during anal contraction at the end of defecation. These are attributed to small
57 mammals such as Sciuridae and/or Chiropteridae. Overall, these data provide new insights into
58 the diversity of post-Mesozoic coprolites and refine our understanding of their producers and
59 associated ecosystems in Central Europe.

60

61 **Keywords:** terrestrial and marine bromalites, coprolites, faeces, Oligocene, Miocene, Poland.

62

63 Introduction

64

65 The oldest known vertebrate coprolites date back to the Ordovician (e.g., *Hunt*
66 & *Lucas*, 2012). However, most published data on coprolites pertain to the Mesozoic era (e.g.,
67 *Eriksson et al.*, 2011; *Salamon et al.*, 2012; *Schweigert & Dietl*, 2012; *Brachaniec et al.*, 2015;
68 *Schwimmer et al.*, 2015; *Zatoń et al.*, 2015; *Niedźwiedzki et al.*, 2016; *Vajda et al.*, 2016; *Chin*,
69 *Feldman & Tashman*, 2017; *Segesdi et al.*, 2017; *Barrios-de Pedro et al.*, 2018; *Barrios-de*
70 *Pedro*, *Chin & Buscalioni*, 2020; *Qvarnström et al.*, 2019, 2024; *Lukeneder et al.*, 2020; *Rummy*,
71 *Halaçlar & Chen*, 2021; *Román et al.*, 2024 and literature cited therein).

72 Post-Mesozoic coprolites - or objects interpreted as such - are comparatively less documented.

73 These have been attributed to a range of producers, including giant earthworms, fish, rodents,
74 notoungulates, thylacynid and borhyaenoid marsupials, hyenas and/or hyaenids and
75 barbourfelids, as well as various indeterminate carnivorans, sirenians, and crocodylians. They
76 have been reported from scattered localities across Europe, North and South America, and Asia
77 (e.g., *Wetmore*, 1943; *Amstutz*, 1958; *Edwards*, 1976; *Wilson*, 1987; *Richter & Baszio*, 2001;
78 *Seilacher et al.*, 2001; *Richter & Wedmann*, 2005; *Dvořák et al.*, 2010; *Godfrey & Smith*, 2010;

79 *Peñalver & Gaudant, 2010; Pesquero et al., 2011; Stringer & King, 2012; Hunt & Lucas, 2014;*
80 *Dentzien-Dias et al., 2018; Wang et al., 2018; Collareta et al., 2019; Kapur et al., 2019;*
81 *Tomassini et al., 2019; Abella et al., 2021; Gross et al., 2023; Román et al., 2024).* A
82 comprehensive overview of numerous Quaternary coprolites was provided by *Hunt & Lucas*
83 *(2012)*, and *Wood & Wilmshurst (2014, 2016)*, *Tolar & Galik (2019)*, *Agliano et al. (2024)*, and
84 *Cambraero & García (2024)*; for review see also *Gurjão et al. (2024)* and literature cited
85 therein.

86 The only marine coprolites from post-Mesozoic sediments of Poland were thoroughly described
87 and illustrated by *Bajdek & Bieńkowska-Wasiluk (2020)*, based on material from the Oligocene
88 (Rupelian) of southeastern Poland. These authors documented sixteen coprolites from two
89 localities within deep-water sediments of the Menilite Formation - an interval renowned for its
90 spectacular fossil fish assemblages (e.g., *Bieńkowska, 2004; Kotlarczyk et al., 2006;*
91 *Bieńkowska-Wasiluk, 2010*). *Bajdek & Bieńkowska-Wasiluk (2020)* concluded that the elongated,
92 linear, often strongly sinuous, and occasionally tear-shaped coprolites they described (see table 1
93 and fig. 2 in *Bajdek & Bieńkowska-Wasiluk, 2020*) were most likely produced by carnivorous
94 teleost fish.

95 *Brachaniec et al. (2022)* described 29 lacustrine, excrement-shaped ferruginous masses - referred
96 to as "alleged" coprolites - from the Miocene (Burdigalian) deposits of the Turów lignite mine in
97 southwestern Poland. The latter authors suggested that one of the identified morphotypes, i.e.,
98 sausage-shaped (see fig. 2A, B in *Brachaniec et al., 2022*), was likely produced by a testudinoid
99 turtle, supported by the discovery of a shell fragment at the site. The second morphotype
100 comprised rounded to oval-shaped fecal forms (see fig. 2E–G in *Brachaniec et al., 2022*), which
101 were interpreted as having been produced by snakes, whose remains are abundant in the
102 surrounding area. However, the involvement of other potential producers, such as lizards or
103 crocodiles, could not be ruled out. Finally, *Brachaniec et al. (2022)* emphasized that although
104 less likely, abiotic processes might also have contributed to the formation of these structures.
105 The aim of this study is to describe and systematically analyze numerous coprolites originating
106 from both lacustrine and marine environments in Poland. The marine settings are represented by
107 Oligocene and Miocene sediments from thirteen localities in southeastern Poland, while the
108 studied lacustrine deposits are Miocene in age and come from southwestern, southern,
109 southeastern, and central parts of Poland (*Figure 1*). The coprolites have been categorized into
110 distinct morphotypes. Their mineralogical composition, associated fossil inclusions,
111 palaeoecological context, and the broader palaeobiological significance of the findings are
112 discussed in detail.

113

114 **Geological setting**

115 The field works were carried out in five areas located in southern and central Poland (see *Figure*
116 *1*).

117

118 **Figure 1 around here**

119

120 *Kleszczów Graben area*

121 The Kleszczów Graben is located in central Poland in Łódź Voivodeship; the graben is over 80
122 km long and up to 3 km wide structure ('B' on *Figure 1A*). It is the deepest tectonic depression
123 in the Polish Lowlands as it exceeds 550 m below sea level in depth (*Widera, Klęsk & Urbański,*
124 *2024*). Its bedrock is formed by Permian salts and carbonates of Jurassic to Cretaceous age (e.g.,
125 *Olchowy, Krajewski & Felisiak, 2019*). The tectonic development of the graben began in
126 Cenozoic (Paleocene) and its in-filling sediments experienced three main phases of deformation,
127 including Valachian stage, Bełchatów stage and "upper" stage with galcitronics (*Krzyszowski,*
128 *1989*) and Rupelian (early Oligocene). The palaeotectonic evolution of this graben accelerated
129 following the late Oligocene (Chattian) regional uplift. The lowermost Miocene sediments are
130 siliciclastics consisting of sands, muds, clays, and thin layers of lignite (*Czarnecki, Frankowski*
131 *& Kuszneruk, 1992*). A coal complex of lignite follows these lowermost siliciclastics of Miocene
132 and comprises lenses of non-coal sediments and rocks, including sands, clays, lacustrine chalk,
133 flints, sandstones, and paratonsteins (tuff horizons; *Widera, Klęsk & Urbański, 2024*). The
134 middle Miocene succession ends with clay-coal and clay-sand complexes as seen in the
135 Bełchatów section - these complexes have total thicknesses of up to 100–150 m (*Widera, Klęsk*
136 *& Urbański, 2024*) and provide fossil plant remains and coprolites described herein.

137

138 *Southern Poland (southern edge of the Holy Cross Mountains)*

139 Miocene sediments exposed in the southern edge of the Holy Cross Mountains are located in the
140 marginal, northern part of the Carpathian Foredeep ('C' on *Figure 1A*). This area was located in
141 the northern part of central Paratethys in the Miocene (*Salamon et al., 2024*). The coastal and
142 shallow-marine sediments of the area formed in an environment of moderate environmental
143 energies (*Studencki, 1999*). Occasionally, the sediments were influenced by storms, which
144 resulted in formation of bivalve accumulations with numerous other fossils (*Baluk & Radwański,*
145 *1977; Gutowski, 1984*). Abundant, large foraminifers (*Amphistegina* and *Heterostegina*) are
146 typical for these shallow marine early Badenian Paratethys deposits. No structures indicative of
147 linear currents have been observed, which might be an indication of high turbulence waters
148 during the storms. One coprolite specimen comes from the so-called *Heterostegina* Sands of the
149 Pińczów Formation of Gołuchów locality.

150 Lithified lower Kimmeridgian oolitic-bioclastic limestones are exposed at the Gołuchów site and
151 fine-grained red-algal sandy limestones with isolated pebbles of the same Kimmeridgian oolitic
152 limestones cover them. Above, fine detrital sands and poorly lithified marly sandstones are
153 exposed. They are attributed to *Heterostegina* Sands – sediments with common foraminifers,
154 molluscs, bryozoans, serpulids, echinoderms, and teeth of fish (*Salamon et al., 2024*) **that**
155 **provided the single coprolite specimen documented in this paper.**

156

157 *South-western Poland (Turów area)*

158 The Turów lignite mine ('D' on *Figure 1A*) is located in the south-western part of the Lower
159 Silesia Voivodeship (south-western Poland). It covers former village of Turów (near Bogatynia),
160 in the central part of the mesoregion Żytawa-Zgorzelec Depression located between the state
161 borders of Poland, Czechia and Germany. The thickness of the sediments exposed in the Turów
162 profile is about 250 m. These sediments comprise seven lithostratigraphic units of sedimentary
163 rocks. Most of those units are dominated by clays and/or muds with only minor intercalations of
164 coarser facies, like sands or gravel-bearing sands (*Kasiński et al., 2015*). The oldest Cenozoic
165 sediments of the sedimentary succession exposed herein are Oligocene sediments (Egger age),
166 forming the lower and middle part of the Turoszów Formation (*Kasiński et al., 2015*). There are
167 coal seams in the middle part of the profile. These seams belong to the Opolno and the
168 Biedzychowice Formations, which are the primary deposits exploited by the Turów mine. The
169 coprolites described in the current study have been collected from the upper part of the
170 Biedzychowice Formation (Karpatian, Burdigalian; comp. *Brachaniec et al., 2022*). The
171 youngest sediments are of the Gozdnicza Formation and Pleistocene till of glacial origin. These
172 units are, contrary to the older ones, dominated by sands and gravels (*Kasiński et al., 2015*).

173

174 *South-eastern Poland (Roztocze)*

175 The Roztocze is a geographical region in south-eastern Poland located in the Lubelskie and
176 partly in the Podkarpackie Voivodeships. It connects the Lublin Upland with Podolia in Ukraine
177 ('E' on *Figure 1A*). Miocene sediments of the Roztocze are dated as Badenian and Sarmatian
178 (*Wysocka, Jasionowski & Peryt, 2007*). Although these are marine formations, determining their
179 exact age is challenging due to the peculiarities of the depositional environment and the complex
180 connections between the Pre-Carpathian foredeep basin and the Central and Eastern Paratethys.
181 The use of separate lithostratigraphic schemes by Polish and Ukrainian geologists for cross-
182 border strata further complicates age determinations (*Bogucki et al., 1998*). The investigated
183 Miocene sediments represent diversified shallow-marine and shoreface facies: quartz sands
184 dominate and are overlain by pelitic limestones in the lower part, and quartz-rodoid sands,
185 organodetritic limestones, reef-type organodetritic limestones, shells, marls and serpulid-
186 microbialitic limestones (*Musiał, 1987; Jasionowski, 1997*). Current field investigations focused
187 on four sites (Brusno, Huta Różaniecka, Józefów, and Żelebsko; for details see e.g., *Wysocka,*
188 *Jasionowski & Peryt, 2007*). Coprolites were found in Sarmatian calcarenites with spheroidal
189 bodies of serpulid-microbial limestones at the Żelebsko site.

190

191 *South-eastern Poland (Menilite-Krosno Series of the Outer Carpathians)*

192 The Menilite-Krosno Series of the Outer Carpathians is located in southeastern Poland in the
193 Subcarpathian Voivodeship ('E' on *Figure 1F*). At the Eocene–Oligocene boundary, tectonic
194 activity and eustatic drop of sea level resulted in restriction of contact between sedimentary sub-
195 basin of the Menilite-Krosno Series of the Outer Carpathians (part of the central Paratethys) and
196 larger basin of the eastern Paratethys and of the Mediterranean domain (*Popov et al., 2002*). The
197 Menilite-Krosno Series of Oligocene (Rupelian and Chattian) and Miocene (Aquitanian and

198 Burdigalian) comprise bituminous marlstones, cherts, shales, and sandstones with common fish
199 fossils (e.g., *Bieñkowska-Wasiluk, 2010*). The series is a result of the activity of submarine fans,
200 bottom currents, and deposition from low concentration turbidity currents as well as pelagic
201 sedimentation and blooms of coccolithophores (*Kotlarczyk et al., 2006*). Current fieldworks
202 focused on 24 sites of several hundred listed by *Kotlarczyk et al. (2006) (Table 1, Figure 1)*,
203 which represent both Oligocene and Miocene sediments. The studied coprolites were found in
204 nine of the selected sites (Oligocene: Kąkolówka I, Kąkolówka II, Wola Czudecka, Futoma,
205 Jamna Dolna, Rudawka Rymanowska, Równe, Wujskie, and Jasienica Rosielna; Miocene:
206 Temeszów and Brzuska; for detailed geology and lithology of these localities see *Kotlarczyk et*
207 *al., 2006*).

208

209 **Materials and methods**

210 Collected coprolites are housed in Sosnowiec (Poland) at the Institute of Earth Sciences, Faculty
211 of Natural Sciences of the University of Silesia in Katowice, Poland (hereafter: IES), and
212 catalogued under registration numbers GIUS 10–3796/O/1–300 (for Oligocene) and GIUS 10–
213 3796/M/1–34 (for Miocene). A detailed specimen lists and descriptions are provided in *Tables 1*
214 *and 2*. Fossil fishes from *Figures 10, 13* also have been catalogued as GIUS 10–3796/O/F1–4,
215 GIUS 10–3796V; these specimens are also housed in the IES. Fossil specimens of potential
216 producers illustrated in *Figures 7–9, 11, 12* are from the Museum of Fossils and Minerals,
217 Dubiecko, Poland and have catalog numbers starting with acronyms Kr., MSMD, ROJ, RORR,
218 Ma, ROL, ROJR, ROU, ROM.

219

220 **Tables 1 and 2 around here**

221



222 There have been eighteen (18) coprolites studied from the Kleszczów Graben area (continental
223 Miocene; GIUS 10–3796/M/1–5, 6, 6(1), 6(2), 6(3), 6(4), 6(5), 7–12) and five (5) of those
224 specimens have been selected for detailed investigation in thin sections (GIUS 10–3796/M/1, 2,
225 6,7,11). Turów area (continental Miocene) provided eighteen (18) more specimens (GIUS 10–
226 3796/M/14–31), and three (3) of those have been subjected to further examination in thin
227 sections (GIUS 10–3796/M/17, 20, 27). The single specimen (GIUS 10–3796/M/13) collected
228 from the southern edge of the Holy Cross Mountains (marine Miocene), and another one from
229 Roztocze area (GIUS 10–3796/M/32), have been also selected for thin section analyses. There
230 were 302 coprolites from the Menilite-Krosno Series of the Outer Carpathians (marine Oligocene
231 and Miocene; GIUS 10–3796/O/1–300, GIUS 10–3796/M/33,34), and fifty (50) of those have
232 been designated for detailed further analyses in thin sections (GIUS 10–3796/O/1–47, GIUS 10–
233 3796/O/107, GIUS 10–3796/O/294, GIUS 10–3796/O/300, GIUS 10–3796/M/33,34).
234 Nearly all specimens were macroscopically documented in situ through field photography during
235 field investigations. An exception was the group of elongated specimens with a distinct,
236 prominently pointed end [(*Figure 3M*; GIUS 10–3796/M/6, 6(1), 6(2), 6(3), 6(4), 6(5)]. These
237 were recovered by washing clay samples from the Kleszczów Graben area. Two samples were
238 processed, weighing 40 kg and 45 kg, respectively. These samples were transported to the

239 laboratory in Sosnowiec (Poland) belonging to the IES. The samples were washed using running
240 hot tap water, screened on a sieve column ($\text{\O}3.0$, 1.0, 0.315 and 0.1 mm-mesh respectively), and
241 finally dried at 150°C. This washed, screened and dried residue was observed under a Leica
242 WildM10 microscope in search for vertebrate microremains.

243 The coprolites described in this article have been further investigated with a number of different
244 analytical tools. The methodological details are presented below.

245

246 *Optical microscopy and thin-sectioning*

247 Optical observations of thin sections have been carried out using Leica SZ-630T dissecting
248 microscope and Nikon Eclipse E100 light microscopy, while the microphotographs have been
249 collected using Olympus BX51 – a polarizing microscope equipped with an Olympus SC30
250 camera and a halogen light source (analyses conducted at the IES).

251 Thin sections were made in the Grindery at the IES. Specimens were embedded in Araldite
252 epoxy resin, sectioned, mounted on the microscope slides and polished with silicon carbide
253 and aluminum oxide powders to about 30 μm thick.

254

255 *Scanning electron microscopy*

256 The chemical composition of the coprolite matrix and embedded microfossils have been
257 examined using the desktop scanning electron microscope (SEM) Phenom XL (Phenom World,
258 Thermo Fisher Scientific, Netherlands), equipped with a fully integrated energy-dispersive X-ray
259 spectroscopy (EDS) detector and secondary electron detector (SED), located at the IES. The
260 observations were conducted under low-vacuum conditions with an accelerating voltage of 15
261 kV. Samples were not coated.

262

263 *Microtomography*

264 One representative specimen from each identified morphotype was selected for virtual sectioning
265 (specimens no. GIUS 10–3796/O/2, GIUS 10–3796/O/9, GIUS 10–3796/O/18, GIUS 10–
266 3796/O/21, GIUS 10–3796/O/30, GIUS 10–3796/O/111, GIUS 10–3796/M/3, GIUS 10–
267 3796/M/6, GIUS 10–3796/M/9, GIUS 10–3796/M/12, GIUS 10–3796/M/13, GIUS 10–
268 3796/M/18, GIUS 10–3796/M/21, GIUS 10–3796/M/32, GIUS 10–3796/M/34).

269 In microtomographic studies, the flat shape of the samples in the form of a disc makes it difficult
270 to optimally position them in relation to the radiation source and the detector. Precise positioning
271 is also required so that the X-ray beam penetrates the entire thickness of the sample without
272 losing focus. Incorrect positioning leads to image distortions (artefacts) caused by differences in
273 the thickness of the x-rayed layers and to difficulties in 3D reconstruction due to the limited
274 number of projection angles. Due to these difficulties some of the samples had to be cut using a
275 mini-grinder. The form of columns facilitates imaging using an X-ray scanner.

276 Microtomographic studies were carried out in the Laboratory of Computed Microtomography of
277 the Institute of Biomedical Engineering of the University of Silesia in Katowice. The samples
278 were scanned at voltage parameters of 160 kV and current of 50 μA , 100 μA with resolutions of
279 8 μm , 10 μm and 25 μm . Each projection with a resolution of 2024x2024 pixels consisted of

280 three repetitions with an exposure time of 500 ms. The scanning time of the coprolites was about
281 one hour during which 2100 x-rays were taken.

282 The images after reconstruction were processed using Volume Graphics®VGSTUDIO Max
283 software, where image normalization and appropriate positioning and geometric measurements
284 were performed. Visualization, animations and detailed analysis were performed using the
285 Volume Graphics®myVGL viewer.

286

287 *Observations of extant excrements*

288 For comparative observations, more than 400 feces from contemporary animals were collected
289 over a period of six months. The collected excrements belonged to invertebrates (crabs) and
290 vertebrates (fish, reptiles, birds, and mammals). They were all collected in the animals' natural
291 habitat in the Municipal Zoological Garden in Łódź, Poland. For comparative purposes, we also
292 used archived data on the feces of fish, amphibians, reptiles, birds, and mammals, which were
293 collected in 2021 at the Silesian Zoological Garden in Chorzów, Poland (for details see
294 *Brachaniec et al., 2022*). External and internal features of the fecal masses were analyzed.
295 Particular attention was given to those clades that have representatives in the Oligocene and
296 Miocene sediments of Poland and neighbouring areas, and could therefore have been among the
297 producers responsible for the studied coprolites.

298

299 **Results**

300 *Coprolite morphology*

301 A total of 339 coprolites were collected: 300 from Oligocene and 39 from Miocene sediments
302 (for details see *Table 1* and *2*). Six different morphotypes were distinguished, characterized by
303 different shapes and sizes (sinusoidal; elongated; straight, curved; irregular; S-shaped; and oval);
304 for details see *Tables 1–4, Figures 2–3*.

305



306 **Tables 3 and 4 around here**

307

308 The colours of coprolites varied, even within the same morphotype and age group. Oligocene
309 (M-KS) sinusoidal forms were most often black (51%) and brown (49%). Black (43%), brown
310 (37%), grey (19%), and red (2%) specimens were found also among elongated Oligocene
311 coprolites. The oval and the regular ones were grey (77%), red (21%), and pastel (2%) in colour.
312 The S-shaped coprolites were black (60%), brown (30%), and red (105). Finally, the curved
313 forms were red (70%), brown (25%), and grey (5%).

314 In the case of continental Miocene specimens (Turów area), their colours varied from pale
315 orange, through greenish red, to burgundy-colored. The ferruginous specimens from Kleszczów
316 Graben were celadon, brown-blue, and locally red. Six specimens were light pastel to light
317 brown. Specimens from the marine Miocene of Roztocze area and Gołuchów quarry (the edge of
318 the Holy Cross Mountains) were light orange and light brown, respectively.

319

320 **Figures 2 and 3 around here**

321

322 *Microtomographic, optical and SEM microscopy studies*

323 Microtomographic studies of terrestrial Miocene coprolites did not reveal any well visible
324 internal structures (Movie S1) that could constitute some undigested food remains [(GIUS 10–
325 3796/M/3, GIUS 10–3796/M/6, GIUS 10–3796/M/9, GIUS 10–3796/M/12) – Kleszczów Graben
326 area; (GIUS 10–3796/M/18, GIUS 10–3796/M/21) – Turów area)]. The same is true for three
327 specimens from marine Miocene environments [(GIUS 10–3796/M/13) – Gołuchów quarry in
328 southern edge of the Holy Cross Mountains; (GIUS 10–3796/M/32) – Żelebsko in Roztocze
329 area; (GIUS 10–3796/M/34) – Brzuska locality in Menilite-Krosno Series of the Outer
330 Carpathians]. However, the specimens from Oligocene marine sediments differed in this respect
331 [(GIUS 10–3796/O/2, GIUS 10–3796/O/18, GIUS 10–3796/O/9, GIUS 10–3796/O/21, GIUS
332 10–3796/O/30, GIUS 10–3796/O/111) – in all specimens from Menilite-Krosno Series of the
333 Outer Carpathians, some undigested food remains were observed, and these food item remnants
334 include mostly remains of fish (bones, scales and teeth; see *Supplementary movie 1*).

335 Thin sections made from continental Miocene coprolites were analyzed in transmitted and
336 reflected light. Dark, nearly opaque matrix can be seen in the specimens from Kleszczów Graben
337 area (GIUS 10–3796/M/1, GIUS 10–3796/M/2, GIUS 10–3796/M/7, GIUS 10–3796/M/11) and
338 from Turów area (GIUS 10–3796/M/17, GIUS 10–3796/M/20, GIUS 10–3796/M/27). The
339 mineral matrix is homogeneous and some elongated structures can be observed within it. These
340 elongated features have arcuate shapes in some cases and they appear to be light-reduction areas in
341 reflected light whereas the surrounding matrix was oxidized. The dark (rusty, brown to almost
342 black), slightly transparent colour of the matrix suggests an iron-rich mineral(s) that formed the
343 matrix. No other distinguishable microdebris were observed. A bright matrix can be observed
344 in one specimen when seen under transmitted light [(GIUS 10–3796/M/6) – Kleszczów Graben
345 area]. No biogenic remains were observed in this case, only some indeterminate mineral
346 structures. Similar results of thin section analyses were obtained from the specimens collected
347 from the southern edge of the Holy Cross Mountains (marine Miocene; (GIUS 10–3796/M/13)
348 and Roztocze area (GIUS 10–3796/M/32).

349 A bright and opaque matrix can be observed in thin sections made from the marine Oligocene
350 and Miocene coprolites of the Menilite-Krosno Series of the Outer Carpathians (GIUS 10–
351 3796/O/1–47, GIUS 10–3796/O/107, GIUS 10–3796/O/294, GIUS 10–3796/O/300, GIUS 10–
352 3796/M/33, 34). The matrix is homogeneous in most of the analyzed samples, however in some
353 cases small structures with angular edges can be noted. Numerous fish remains can be observed
354 embedded within the matrix, and these remains, after further examination under SEM (*Figures 4,*
355 *5*), have been found to represent fish bones, scales and teeth. There were no fossil remains of fish
356 or other organisms observed in thin sections made from specimens: GIUS 10–3796/M/33 and
357 GIUS 10–3796/M/34 (Miocene of the Menilite-Krosno Series of the Outer Carpathians).

358

359 **Movie S1 around here**

360

361 **Figure 4 around here**

362

363 *Mineralogical and structural analyses*

364 The chemical composition (SEM) analysis of coprolite no. GIUS 10–3796/M/33 revealed that
365 the coprolite matrix is highly porous and consists of microcrystalline fluorapatite, which occurs
366 in small (about 0.5–4 μm in diameter) thin-walled vesicles. These forms are considered mineral
367 pseudomorphs of organic structures in the original feces (Hollocher *et al.*, 2010). Some
368 researchers suggest that this specific structure is associated with spherical bacteria, such as
369 *Enterococcus faecalis*, and other common cocci found in feces (Hollocher *et al.*, 2010). It has
370 also been shown that under natural conditions and in laboratory experiments, bacteria, and even
371 their phosphatases, can promote the precipitation of microcrystalline apatite (Hirschler, Lucas &
372 Hubert, 1990; Lucas & Prévôt, 1991; Jehl & Rougerie, 1995), which suggests that the fecal
373 bacteria themselves may have been involved in the apatite mineralization process (Hollocher *et*
374 *al.*, 2010). There are fragments embedded within the porous matrix that have lower porosity and
375 are composed of fluorapatite of clearly organic origin (Figures 4,5). These microfossils most
376 likely represent bone fragments, teeth, and remnants of plant tissues. Additionally, the matrix
377 contained mineral grains such as quartz and zircon, as well as crystals that had formed within the
378 voids of the coprolites, including calcite and framboidal pyrite. The only coprolite with a
379 different chemical composition was one specimen from Turów. This specimen had also porous
380 matrix structure but it consists of iron oxides and hydroxides. No microfossils were found within
381 it.

382

383 **Figure 5 around here**

384

385 *Contemporary comparative studies*

386 The visual comparison made it possible to exclude modern feces that differed significantly from
387 the analyzed coprolites in terms of size and shape. These feces samples were not taken into
388 account in further analyses. The subsequent observations were based on a morphological
389 comparison between the selected recent feces and the studied coprolites. Surprisingly, crabs
390 (*Coenobita brevimanus*) were observed to produce fecal masses of sinusoidal morphology
391 (Figure 6J) similar to coprolites described by us from the Oligocene (see e.g., Figures 2C-E,
392 3B). Nearly identical sinusoidal feces (see Figure 6K) were produced by another crab (flying
393 crab, *Liocarcinus holsatus*), which is closely related to fossil representatives of *Liocarcinus* – a
394 taxon commonly found in the Menilite-Krosno Series of the Outer Carpathians. So far, this type
395 of coprolite morphology has been attributed to predatory fishes (e.g., Bajdek & Bienkowska-
396 Wasiluk, 2020). However, despite the examination of numerous faces produced by extant fish
397 taxa (a total of 30 species belonging to Scombriformes and Gadiformes), no corresponding
398 sinusoidal morphology has been observed in the fecal remains of any of these taxa. The observed
399 recent feces of studied fish taxa were dominated by masses with morphologies resembling
400 coprolites' morphologies classified into straight, curved, and S-shaped categories (see Figure

401 6N). These fish-produced fecal masses comprised various remains of other, presumably
402 consumed fish individuals (bones, scales, teeth). Noteworthy, the studied coprolites with similar
403 morphologies also contain fossil fish remnants.
404 Current observations show that barracudas produce more or less regular feces, sometimes
405 slightly tapering on one side (comp. *Figure 6I*). There is a similar morphological type in the
406 studied sample of Oligocene coprolites (more or less regular with macroscopically visible
407 vertebrate remains; *Figures 2O, 3C*). It is likely, based on morphologic and size criteria, that this
408 fossil coprolite specimen was also produced by barracuda (*Sphyræna*).
409 Oval and relatively large coprolites from the Oligocene marine sediments (*Figure 2U*) do not
410 contain any faunal remains. Their shape and size resemble the fecal masses produced by
411 members of the bird family Columbidae (*Figure 6H*). Noteworthy, fossil remains of these birds
412 have been documented in the Menilite-Krosno Series of the Outer Carpathians (*Bocheński,*
413 *Tomek & Świdnicka, 2010*).
414 Deep-sea coprolites documented from the Miocene deposits are represented by relatively long
415 and complex faecal masses consisting of string with frequent constrictions (*Figure 3D*). These
416 fossil specimens have morphology most closely resembling feces of holothurians (*Holothuria*
417 *sp.*; *Figure 6L*) and cephalopods (*Nautilus pompilius*; *Figure 6M*).
418 The last type of bromalites compared with recent fecal masses consists of phosphatic specimens
419 recovered from continental Miocene strata. These coprolites are elongated and exhibit a
420 characteristic, prominently pointed end, likely formed as the anus contracted to close and sever
421 the expelled fecal mass (*Figure 3M*). Among vertebrates inhabiting the present-day terrestrial
422 environments of central Poland, the feces of Sciuridae and Chiropteridae are most comparable to
423 the fossil specimens, as they are similarly small and display a distinct pointed termination at one
424 end (*Figures 6D, E*).

425

426 **Figure 6 around here**

427

428 **Discussion**429 *Oligocene marine coprolites*

430 Majority of the currently documented coprolites come from the Oligocene sediments of the
431 Menilite-Krosno Series of the Outer Carpathians in southern Poland (for details see *Table 1*).
432 *Bajdek & Bieńkowska-Wasiluk (2020)* argued that the high abundance of mesobathypelagic fish
433 remains documented in these sediments may point to a well-oxygenated deep-marine
434 environment (likely exceeding 500 m in some places). *Kotlarczyk et al. (2006)* concluded that
435 the basin depth in this area could have been even greater, locally exceeding 2,000 m. The
436 coprolites from these deep marine facies were classified into five morphotypes. The first type,
437 characterized by a sinusoidal shape, was previously recorded from Oligocene strata in southern
438 Poland (*Bajdek & Bieńkowska-Wasiluk, 2020*). These authors concluded that these coprolites
439 were produced by fish predators, mainly representatives of *Palimphyes*, *Oligophus*, and an
440 indeterminate gadiform. However, current experimental studies suggest that similar faecal

441 morphologies could also be associated with invertebrates, such as crabs, whose fossils are
442 relatively common in the Menilite-Krosno Series (*Jerzmańska, 1967; Bieńkowska-Wasiluk,*
443 *2010; Figure 7*). Although *Bajdek & Bieńkowska-Wasiluk (2020)* considered crabs as potential
444 producers, they ultimately ruled them out, reasoning that the crabs known from these strata were
445 too small to produce long, sinusoidal coprolites. Noteworthy, the lengths of faecal strings may
446 approach the body lengths of their producers. Furthermore, when estimating producer size, the
447 total faecal mass or the diameter of the coprolite may serve as more reliable indicators of the
448 producer's body size or anus size, respectively, than the length of faecal strings (see *Donovan,*
449 *1994*). Our experimental studies demonstrate that crabs are capable of producing long faecal
450 strings with sinusoidal morphologies comparable to those observed in the studied fossil
451 coprolites (cf. *Figure 2A-E* and *Figure 6K*).

452 We suggest that the three successive morphotypes, i.e., straight, curved with macroscopically
453 visible vertebrate remains, and S-shaped, were produced by fish (see *Figures 8-11*).
454 Morphologically similar non-spiral coprolites (e.g., *Figure 2F-J*) are known from the Eocene
455 deposits of the Green River Formation (*Edwards, 1976*), the Coldwater Beds (*Wilson, 1987*), and
456 Messel (*Richter & Wedmann, 2005*). Rope-like (non-spiral) faecal masses are commonly
457 produced by teleost fishes (see *Figure 6N*), representatives of which inhabited the Oligocene
458 marine environments in southern Poland. Furthermore, our experimental studies indicate that
459 barracudas may produce more or less regular faecal strings, sometimes terminating in a slightly
460 tapering end (cf. *Figure 6I*). Noteworthy, *Kotlarczyk et al. (2006)* also reported the presence of
461 barracudas in the Polish Carpathians.

462 Identifying the producer of the oval coprolite (*Figure 2U*) is challenging. None of the marine
463 taxa known from the Menilite-Krosno Series sediments could be easily linked to this
464 morphology based on current experimental results. However, the morphology and size of the
465 coprolite resemble, to some extent, the excrements of some birds, particularly pigeons
466 (Pigeonidae). Noteworthy, the remains of these birds have been reported from Carpathian
467 sediments (*Bocheński, Tomek & Świdnicka, 2010*). However, before this interpretation can be
468 further substantiated, a thorough taphonomic analysis of the preservation pathway of bird faeces
469 in marine deposits is required. *Bocheński, Tomek & Świdnicka (2010)* also reported fossils of
470 humming birds and some passerines from the same strata. However, the shape and size of the
471 faeces of these taxa differ from those of the studied coprolites (*Bocheński & Bocheński, 2008;*
472 *Bocheński et al., 2011; see Figure 6F*).

473

474 **Figures 7-12 around here**

475

476 *Miocene marine coprolites*

477 Four coprolites were recorded in the marine Miocene sediments (for details see *Table 4*). Two of
478 them (GIUS 10–3796/M/13, 32; *Figure 3E, F*) come from shallow marine deposits displaying
479 high variation of lithologies, facies, and thicknesses (Roztocze area and southern edge of the
480 Holy Cross Mountains). There have been no predatory vertebrates documented in the Żelebsko
481 quarry (Roztocze area) that could have been responsible for the production of the documented

482 apatite faeces. The dominant species at the site are gastropods, bivalves, and foraminifers.
483 However, fossil fish teeth are common in a nearby Gołuchów quarry exposing the sediments of
484 the same age (southern edge of the Holy Cross Mountains). These fossils co-occur at the site
485 with fossils of invertebrates, including foraminifers, molluscs, bryozoans, serpulids, echinoderms
486 (asteroids, echinoids and stalked crinoids (*Salamon et al., 2024*). Most of the fish teeth at the site
487 represent teleost fish (above 70% collected specimens; *Salamon et al., 2024*). They belonged to
488 the family Sparidae. There have been also shark teeth, but those were less numerous, and
489 belonged mainly to the Odontaspidae family, including *Carcharias acutissima* and
490 *Araloselachus cf. vorax*. *Salamon et al. (2024)* also documented shark teeth (68% of all
491 specimens), belonging to at least four families, in the nearby locality of Zygmontów near Książ
492 Wielki (see fig. 2 in *Salamon et al., 2024*). Fossil teeth assigned to *Otodus megalodon*,
493 *Cosmopolitodus hastalis*, *Isurus*, and *Galeocerdo* were found thereas well; myliobatoid teeth
494 were also occasionally noted (*Aetobatus*). According to *Salamon et al. (2024)* teleost fish teeth
495 and tooth plates constitute 24% of the collected teeth specimens, and are represented only by
496 Sparidae. A logical step in the challenging task of producer identification would be to seek
497 potential candidates among predatory taxa represented by fossil teeth. The identification,
498 however, is further complicated by the absence of recognizable faunal remains within the
499 coprolite matrix. The list of potential producer candidates can be even longer as other predatory
500 vertebrates (toothed and toothless cetaceans, porpoises) have been recognized in the northern
501 (Polish) part of Miocene Paratethys (*Czyżewska & Radwański, 1991* and literature cited therein).
502 These mammals cannot be excluded as the potential producers of coprolites from Żelebsko and
503 Gołuchów. *Baluk (1977)* documented numerous remains of cephalopods within the Korytnica
504 Clays of the southern margin of the Holy Cross Mountains. However, the morphology of fossil
505 and extent faeces assignable to these invertebrates (comp. *Knaust & Hoffmann, 2020*, and
506 literature cited therein) differ from the coprolites from Żelebsko and Gołuchów.
507 Two coprolites (GIUS 10–3796/M/33, 34; *Figure 3D*) have been collected from the Menilite-
508 Krosno Series (The Outer Carpathians, Poland) – strata representing marine environment,
509 probably exceeding 500 m depth (*Bajdek & Bienkowska-Wasiluk, 2020*). These are relatively
510 long and complex faecal masses, each consisting of string with frequent constrictions. These
511 features make them similar to the faeces of extent sea cucumbers and cephalopods (see fig. 6, 7
512 in *Knaust & Hoffmann, 2020; Figure 6L, M*). However, holothurians have not been described so
513 far from the Menilite-Krosno Series, and only a single cephalopod specimen has been described
514 from the strata (*Świdnicka, 2007*). Therefore, identification of potential producers must remain
515 speculative as body fossil record is missing or not sufficient. No fossil remains of consumed taxa
516 have been found in the faecal matrix, hindering the producer identification even more
517 problematic.

518

519 *Miocene continental coprolites*

520 There are excrement-like masses (pellets) that are frequently recorded from various clayey
521 sediments (for review see *Brachaniec et al., 2022*). However, some researchers rule out

522 zoological origin of those pellets, despite their superficial similarity to faecal masses. The main
523 characteristics cited against the biological origins of those, are: their ferruginous composition,
524 variation in size, lack of internal inclusions, and scarcity of associated (embedded) vertebrate
525 remains (e.g., *Roberts, 1958; Dake, 1960; Danner, 1994, 1997; Spencer & Tuttle, 1980; Love &*
526 *Boyd, 1991; Spencer, 1993, 1997; Hardie, 1994; Mustoe, 2001*).

527 Several hypotheses have been proposed to explain the origin of these problematic masses,
528 including: co-seismic liquefaction, sediment intrusion into hollow logs or between plant stems,
529 expulsion of sediment under gravitational pressure, and siderite extrusion driven by
530 methanogenesis (*Spencer & Tuttle, 1980; Love & Boyd, 1991; Spencer, 1993; Peterson &*
531 *Madin, 1997; Mustoe, 2001*). However, there have been also a few authors who interpreted these
532 masses as biological in nature, either as fossil faeces (coprolites), cololites, or eviscerolites
533 (*Amstutz, 1958; Broughton, Simpson & Whitaker, 1977; Broughton, Simpson & Whitaker, 1978;*
534 *Seilacher et al., 2001; Broughton, 2017; Brachaniec et al., 2022*). Recently, *Brachaniec et al.*
535 *(2022)* presented a detailed study of excrement-shaped ferruginous masses from the Miocene
536 strata of Poland (Turów, south-west Poland). The authors described two coprolite morphotypes:
537 the first includes small, sausage-shaped specimens, while the second comprises larger, more
538 rounded to oval, massive specimens with a rough surface, sometimes exhibiting a prominent
539 pointed end covered by a striated pattern, interpreted as a morphology resulting from anal
540 contraction during the cutting off of the expelled portion of the faecal mass. The latter authors
541 combined their palaeontological and mineralogical analytical results with experimental data and
542 concluded that these structures may represent “true” coprolites, which were likely produced by
543 reptiles [smaller morphotype – by tortoises (*Testudinoidea*)] and larger one – by snakes
544 (*Serpentes*)]. This conclusion was supported by the morphological match between the fossil and
545 experimental faecal masses (including fine striations), as well as by the presence of hair-like
546 structures (or coalified inclusions) within the coprolites, which could suggest a diet including
547 mammals.

548 In the current study (see Table 4) we documented thirty (30) ferruginous coprolites (GIUS 10–
549 3796/M/1–12, 14–31). These specimens have been collected from two regions of southern
550 Poland (the Turów area and the Kleszczów Graben area). All these coprolites are represented by
551 one morphotype only (II morphotype sensu *Brachaniec et al., 2022*; i.e., more rounded to oval,
552 elongate, massive specimens with rough surface; *Figure 3G-L, N*). These coprolites comprise
553 numerous hair-like structures, coalified inclusions, and traces of fine striations visible on the
554 surfaces. These features make them similar to other Miocene coprolites ascribed so far to snakes
555 (fig. 2H-M in *Brachaniec et al., 2022*). However, other producers cannot be ruled out
556 definitively at this stage. A rich assemblages of continental tetrapod fauna have been
557 documented from slightly older sediments (Eocene and Oligocene) of surrounding areas (north-
558 western Bohemia and south-eastern Germany). *Brachaniec et al. (2022)* mentioned other fossil
559 representatives, including frogs, salamanders, choristoderans, crocodiles, turtles, lizards, and
560 snakes from these regions (for details see table 1 in *Brachaniec et al., 2022*). The same authors
561 noted that vertebrate fossil remains are abundant in the Miocene of northern Bohemia (North

562 Bohemian Brown Coal Basin in Czechia), and are represented by osteichthyan fish, amphibians,
563 reptiles, birds, and mammals, among others (for details see table 2 in *Brachaniec et al., 2022*).
564 Rodents of Sciuridae family could be responsible for the apatite coprolites with a characteristic
565 and prominent pointed termination, that likely formed due to contraction of anus closing to cut
566 off the faecal mass (GIUS 10–3796/M/6, 6(1), 6(2), 6(3), 6(4), 6(5); *Figure 3M*). Such coprolites
567 have been found in the sediments of the Kleszczów Graben area (*Garapich, 2002; Kowalski &*
568 *Rzebik-Kowalska, 2002*). *Chame (2003)* studied excrements of extant mammals and illustrated
569 small (max. length 1.5 cm) faeces, with a narrowing termination (see table 1 in *Chame, 2003*).
570 This type of faeces was produced by Sciuridae (*Chame, 2003*). Alternatively, it is also possible
571 that representatives of Chiropteridae produced this type of coprolites from the Kleszczów Graben
572 – indeed their fossil remains in the strata have been documented by *Garapach (2002; see also*
573 *Figure 13)*.
574 The current actualistic studies show that bat (*Carollia perspicillata*) may produce elongated
575 faeces with a characteristic prominent pointed end formed during anus closing (*Figure 6E*). The
576 bat faeces resemble some of the studied fossil specimens (cf. *Figure 3M*). Based on the
577 combination of morphology and size, we exclude the possibility that this type of coprolite was
578 produced by representatives of Talpidae, Castoridae, Caviidae, or lizards, despite the presence of
579 their fossils in the sedimentary strata of the Kleszczów Graben (*Garapich, 2002* and literature
580 cited therein; comp. *Figure 6* and data presented in *Brachaniec et al., 2021*).
581 Other groups of organisms recorded from this area are malacofauna (*Stworzewicz, 1999*), fish
582 (*Kovalchuk et al., 2019*), and crustaceans (*Dumont et al., 2020*). During fieldwork, we
583 documented also other co-occurring fossils represented by bone elements, vertebrae, teeth, and
584 otoliths of freshwater fish belonging to Gobioidae, Umbridae, Cyprinidae, Pleuronectoidae,
585 Apogonidae and "*Anguilloides*" sp. (an extinct relative of an eel). However, the robust
586 morphology (including the pointed termination) and size make representatives of these groups
587 rather unlikely candidates for the producers of the studied ferruginous coprolites.

588

589 **Figure 13 around here**

590

591 **Supplemental Information**592 A movie showing the internal structure of a selected Oligocene (Rupelian) coprolite of the
593 Kąkolówka locality, southern Poland (specimen no. GIUS 10–3796/O/9).

594

595 **ADDITIONAL INFORMATION AND DECLARATIONS**

596

597 **Author Contributions**

598

599 **Tomasz Brachaniec** designed research, analyzed the data, prepared figures and/or tables, and
600 approved the final draft.

601 **Dorota Środek** performed the mineralogical analyses, analyzed the data, prepared figures, and
602 approved the final draft.

603 **Mateusz Salamon** conducted field works and acquired a specimen for research.

604 **Michał Bugajski** conducted field works and acquired a specimen for research.

605 **Piotr Duda** performed the microtomographic studies.

606 **Adam Danielak** performed photos of recent faeces.

607 **Magdalena Janiszewska** performed photos of recent faeces.

608 **Grzegorz Sadlok** analyzed the data and approved the final draft.

609 **Wojciech Kuśnierczyk** conducted field works and acquired a specimen for research.

610

611 **Competing Interests**

612 The authors declare that they have no competing interests.

613

614 **Data availability**

615 All data generated or analysed during this study are included in this published article. For the
616 purpose of Open Access, the first author has applied a CC-BY public copyright licence to any
617 Author Accepted Manuscript (AAM) version arising from this submission.

618

619 **Funding**

620 This research was funded in whole by the National Science Centre, Poland (www.ncn.gov.pl),
621 grant no. 2023/49/B/ST10/00322 for Tomasz Brachaniec.

622

623 **Acknowledgements**

624 Journal reviewers and editor are acknowledged for improving the quality of this study. Special
625 thanks are due to the all employees and authorities of Municipal Zoological Garden in Łódź,
626 Poland, thanks to whom it was possible to carry out actualistic research. Authors thanks to
627 Tomasz Janiszewski for photos of bird faeces, zoological shop “Rybka” for fish faeces, Robert
628 Szybiak for lending some of the specimens for research, and Wojciech Krawczyński for photo
629 documentation. Maciej Pindakiewicz and Adiel A. Klompmaker are acknowledged for otholits and
630 crabs assignation.

631

632 **References**

633

634 **Abella J, Martin-Perea DM, Valenciano A, Hontecillas D, Montoya P, Morales J. 2021.**

635 Coprolites in natural traps: direct evidence of bone-eating carnivorans from the Late
636 Miocene Batallones-3 site, Madrid, Spain. *Lethaia* **54**:762-774 DOI 10.1111/let.12438.

637 **Agliano F, Velázquez NJ, Martínez Tosto AC, Camiolo IS, Rindel DD. 2024.** Camelid diet
638 through microhistological and palynological analyses of feces and coprolites from Parque
639 Nacional Perito Moreno, Patagonia, Argentina. *Journal of Archaeological Science:
640 Reports* **58**:104713 DOI 10.1016/j.jasrep.2024.104713.

- 641 **Amstutz G. 1958.** Coprolites: a review of the literature and a study of specimens from Southern
642 Washington. *Journal of Sedimentary Petrology* **28**:498-508 DOI 10.1306/74d7084e-2b21-
643 11d7-8648000102c1865d.
- 644 **Bajdek P, Bieńkowska-Wasiluk M. 2020.** Deep-sea ecosystem revealed by teleost fish
645 coprolites from the Oligocene of Poland. *Palaeogeography, Palaeoclimatology,*
646 *Palaeoecology* **540**:109546 DOI 10.1016/j.palaeo.2019.109546.
- 647 **Bałuk W. 1977.** A new species of the cuttlefish from the Korytnica Clays (Middle Miocene;
648 Holy Cross Mountains, Poland). *Acta Geologica Polonica* **27**:169-176
- 649 **Bałuk W, Radwański A. 1977.** Organic communities and facies development of the Korytnica
650 Basin (Middle Miocene; Holy Cross Mountains, Central Poland). *Acta Geologica Polonica*
651 **27**:85-123
- 652 **Barrios-de Pedro S, Poyato-Ariza FJ, Moratalla JJ, Buscalioni AD. 2018.** Exceptional
653 coprolite association from the Early Cretaceous continental Lagerstätte of Las Hoyas,
654 Cuenca, Spain. *PloS ONE* **13**:e0196982 DOI 10.1371/journal.pone.0196982.
- 655 **Barrios-de Pedro S, Chin K, Buscalioni AD. 2020.** The late Barremian ecosystem of Las
656 Hoyas sustained by fishes and shrimps as inferred from coprofabrics. *Cretaceous Research*
657 **110**:104409 DOI 10.1016/j.cretres.2020.104409.
- 658 **Bieńkowska M. 2004.** Taphonomy of ichthyofauna from an Oligocene sequence (Tylawa
659 Limestones horizon) of the Outer Carpathians. Poland. *Geological Quarterly* **48**:181-192
- 660 **Bieńkowska-Wasiluk M. 2010.** Taphonomy of Oligocene teleost fishes from the Outer
661 Carpathians of Poland. *Acta Geologica Polonica* **60**:479-533
- 662 **Bocheński Z., Bocheński ZM. 2008.** An Old World hummingbird from the Oligocene: a new
663 fossil from Polish Carpathians. *Journal of Ornithology* **149**:211-216 DOI 10.1007/s10336-
664 007-0261-y.
- 665 **Bocheński ZM, Tomek T, Świdnicka E. 2010.** A columbid-like avian foot from the Oligocene
666 of Poland. *Acta Otnithologica* **45**:233-236 DOI 10.3161/000164510X551363.
- 667 **Bocheński ZM, Tomek T, Bujoczek M, Wertz K. 2011.** A new passerine bird from the early
668 Oligocene of Poland. *Journal of Ornithology* **152**:1045-1053 DOI 10.1007/s10336-011-
669 0693-2.
- 670 **Bogucki A, Gerasimow L, Wołoszyn P, Wysocka A. 1998.** *Budowa geologiczna Roztocza*
671 *Ukraińskiego*. Przewodnik LXIX Zjazdu PTG: Lublin. 245-256
- 672 **Brachaniec T, Niedźwiedzki R, Surmik D, Krzykowski T, Szopa K, Gorzelak P, Salamon**
673 **MA. 2015.** Coprolites of marine vertebrate predators from the Lower Triassic of southern
674 Poland. *Palaeogeography, Palaeoclimatology, Palaeoecology* **435**:118-126 DOI
675 10.1016/j.palaeo.2015.06.005.
- 676 **Brachaniec T, Środek D, Surmik D, Niedźwiedzki R, Georgalis GL, Płachno BJ, Duda P,**
677 **Lukeneder A, Gorzelak P, Salamon MA. 2022.** Comparative actualistic study hints at
678 origins of alleged Miocene coprolites of Poland. *PeerJ* **10**:e13652 DOI
679 10.7717/peerj.13652.
- 680 **Broughton PL. 2017.** Enigmatic origin of massive late Cretaceous-to-Neogene coprolite-like

- 681 deposits in North America: a novel palaeobiological alternative to inorganic
682 morphogenesis. *Lethaia* **50**:194-216 DOI 10.1111/let.12186.
- 683 **Broughton PL, Simpson F, Whitaker SH. 1977.** Late Cretaceous coprolites from southern
684 Saskatchewan: comments on excretion, plasticity and ichnological nomenclature. *Bulletin*
685 *of Canadian Petroleum Geology* **25**:1097-1099
- 686 **Broughton PL, Simpson F, Whitaker SH. 1978.** Late Cretaceous coprolites from Western
687 Canada. *Palaeontology* **21**:443-453
- 688 **Cambroner I, García N. 2024.** Does size matter? Morphological and content analysis of the
689 coprolites from a Quaternary deposit in the Iberian Peninsula. *Quaternary Environments*
690 *and Humans* **2**:100009 DOI 10.1016/j.qeh.2024.100009.
- 691 **Chame M. 2003.** Terrestrial mammal feces: a morphometric summary and description.
692 *Memórias do Instituto Oswaldo Cruz* **98 (Suppl. I)**:71-94 DOI 10.1590/S0074-
693 02762003000900014.
- 694 **Chin K, Feldmann RM, Tashman JN. 2017.** Consumption of crustaceans by megaherbivorous
695 dinosaurs: dietary flexibility and dinosaur life history strategies. *Scientific Reports* **7**:11163
696 DOI 10.1038/s41598-017-11538-w.
- 697 **Collareta A, Gemelli M, Varola A, Bianucci G. 2019.** Trace fossils on a trace fossil: A
698 vertebrate-bitten vertebrate coprolite from the Miocene of Italy. *Neues Jahrbuch für*
699 *Geologie und Paläontologie, Abhandlungen* **293**:117-126 DOI 10.1127/njgpa/2019/0834.
- 700 **Czarnecki L, Frankowski R, Kuszneruk J. 1992.** Synthetic lithostratigraphic profile of
701 Tertiary deposits of the Bełchatów deposit. In: Lipiarski I, ed. *Geologia formacji*
702 *węglonośnych Polski*. Wydawnictwo Akademii Górniczo-Hutniczej: Kraków. 18-23
- 703 **Czyżewska T, Radwański A. 1991.** Middle Miocene (Badenian) delphinid and phocoenid
704 remains from the Fore-Carpathian Depression in southern Poland. *Acta Geologica*
705 *Polonica* **41**:183-191
- 706 **Dake HC. 1960.** Washington coprolites again. *Mineralogist* **28**:2-6
- 707 **Danner WR. 1994.** The pseudocoprolites of Salmon Creek, Washington. University of British
708 Columbia Department of Geological Sciences Report.
- 709 **Danner WR. 1997.** The pseudocoprolites of Salmon Creek, Washington.
- 710 **Dentzien-Dias P, Carrillo-Briceño JD, Francischini H, Sánchez R. 2018.** Paleoecological
711 and taphonomical aspects of the late Miocene vertebrate coprolites (Urumaco Formation)
712 of Venezuela. *Palaeogeography, Palaeoclimatology, Palaeoecology* **490**:590-603 DOI
713 10.1016/j.palaeo.2017.11.048.
- 714 **Donovan SK. 1994.** The palaeobiology of vertebrate coprolites. In: Donovan, SK. ed. *The*
715 *Palaeobiology of Trace Fossils*. John Wiley & Sons Ltd.: Chichester. 221-239
- 716 **Dumont HJ, Pociecha A, Zawisza E, Szeroczyńska K, Worobiec E, Worobiec G. 2020.**
717 Miocene cladocera from Poland. *Scientific Reports* **10**, 12107 DOI 10.1038/s41598-020-
718 69024-9.
- 719 **Dvořák Z, Mach K, Prokop J, Knor S. 2010.** *Třetihorní fauna severočeské hnědouhelné*
720 *pánve*. Prague: Nakladatelství Granit.

- 721 **Edwards P. 1976.** *Fish Coprolites from Fossil Butte, Wyoming*. Wyoming: Contributions to
722 Geology.
- 723 **Eriksson, ME, Lindgren J, Chin K, Månsby U. 2011.** Coprolite morphotypes from the Upper
724 Cretaceous of Sweden: novel views on an ancient ecosystem and implications for coprolite
725 taphonomy. *Lethaia* **44**:455-468 DOI 10.1111/j.1502-3931.2010.00257.x.
- 726 **Garapich A. 2002.** An overview of Miocene rodents from Belchatów (Poland). *Folia Zoologica*
727 **51 (Suppl. 1)**: 59-66
- 728 **Godfrey JS, Smith BJ. 2010.** Shark-bitten vertebrate coprolites from the Miocene of Maryland.
729 *Naturwissenschaften* **97**:461-467 DOI 10.1007/s00114-010-0659-x.
- 730 **Gross M, Prieto J, Grímsson F, Bojar HP. 2023.** Hyena and ‘false’ sabre-toothed cat
731 coprolites from the late Middle Miocene of south-eastern Austria. *Historical Biology* **36**:
732 1903-1922 DOI 10.1080/08912963.2023.2237979.
- 733 **Gurjão L, Dias O, Neto J, Iñiguez A. 2024.** Coprolite diversity from the archeological site
734 Gruta Do Gentio Ll, Unai, Minas Gerais, Brazil. *The Holocene* **34**:1765-1774 DOI
735 10.1177/09596836241275019.
- 736 **Gutowski J. 1984.** Sedimentary environment and synecology of macrobenthic assemblages of
737 the marly sands and red-algal limestones in the Korytnica Basin (Middle Miocene; Holy
738 Cross Mountains, Central Poland). *Acta Geologica Polonica* **34**:323-340
- 739 **Hardie JK. 1994.** Dolomite and siliciclastic dikes and sills in marginal-marine Cretaceous coals
740 of central Utah. *U.S. Geological Survey Bulletin* **2087**:1-19
- 741 **Hirschler A, Lucas J, Hubert JC. 1990.** Apatite genesis: A biologically induced or biologically
742 controlled mineral formation process?. *Geomicrobiology Journal* **7**:47-56
- 743 **Hollocher KT, Hollocher TC, Keith Rigby Jr.J. 2010.** A Phosphatic Coprolite Lacking
744 Diagenetic Permineralization From The Upper Cretaceous Hell Creek Formation,
745 Northeastern Montana: Importance Of Dietary Calcium Phosphate In Preservation. *Palaios*
746 **25**:132-140 DOI 10.2110/palo.2008.p08-132r.
- 747 **Hunt AP, Lucas SG. 2012.** Classification of vertebrate coprolites and related trace fossils. *New*
748 *Mexico Museum of Natural History and Science Bulletin* **57**:137-146
- 749 **Hunt AP, Lucas SG. 2014.** Jurassic vertebrate bromalites of the western United States in the
750 context of the global record. *Volumina Jurassica* **12**:151-158 DOI 10.5604/17313708
751 .1130139.
- 752 **Jasionowski M. 1997.** Zarys litostratygrafii osadów miocénkich wschodniej części zapadliska
753 przedkarpacciego. *Biuletyn Państwowego Instytutu Geologicznego* **373**:43-60
- 754 **Jehl C, Rougerie F. 1995.** Phosphatogenese en atolls polynesiens: La filiation mattes
755 cyanobacteriennes-phosphorites. *Oceanologica Acta* **18**:79-93
- 756 **Jerzmańska A. 1967.** Crabs of the genus *Portunus* Weber from the Menilite Series of the
757 Carpathians. (In Polish, English summmary). *Annales de la Société Géologique de Pologne*
758 **37**:539-545

- 759 **Kapur VV, Kumar K, Morthekai P, Chaddha AS. 2019.** Palaeodiet of Miocene producer(s)
760 and depositional environment(s): inferences from the first evidence on microcoprolites
761 from India. *Acta Geologica Sinica* **94**:1574-1590 DOI 10.1111/1755-6724.14293.
- 762 **Kasiński JR, Badura J, Pańczyk M, Pécskay Z, Saternus A, Słodkowska B, Urbański P.**
763 **2015.** Osady paleogeńskie w polskiej części niecki żytańskiej-nowe światło na problem
764 wieku zapadliska tektonicznego. *Biuletyn Państwowego Instytutu Geologicznego* **461**:295-
765 324 DOI 10.5604/08676143.1142104.
- 766 **Knaust D, Hoffmann R. 2020.** The ichnogenus *Lumbricaria* Munster from the Upper Jurassic
767 of Germany interpreted as faecal strings of ammonites. *Papers in Palaeontology* **7**:807-823
768 DOI 10.1002/spp2.1311.
- 769 **Kotlarczyk J, Jerzmańska A, Świdnicka E, Wiszniowska T. 2006.** A framework of
770 ichthyofaunal ecostratigraphy of the Oligocene-Early Miocene strata of the Polish Outer
771 Carpathian basin. *Annales Societatis Geologorum Poloniae* **76**:1-111
- 772 **Kovalchuk O, Nadachowski A, Świdnicka E, Stefaniak K. 2019.** Fishes from the Miocene
773 lacustrine sequence of Bełchatów (Poland). *Historical Biology* **32**:1011-1018 DOI
774 10.1080/08912963.2018.1561671.
- 775 **Kowalski K, Rzebik-Kowalska B. 2002.** Paleoecology of the Miocene fossil mammal fauna
776 from Bełchatów (Poland). *Acta Theriologica* **47, Suppl. 1**:115-126 DOI
777 10.1007/BF03192483.
- 778 **Krzyszczkowski D. 1989.** The tectonic deformation of Quaternary deposits within the Kleszczów
779 Graben, central Poland. *Tectonophysics* **163**:285-287 DOI 10.1016/0040-1951(89)90263-1.
- 780 **Love JD, Boyd DW. 1991.** Pseudocoprolites in the Mowry Shale (Upper Cretaceous),
781 Northwest Wyoming. *University of Wyoming Contribution to Geology* **28**:139-144
- 782 **Lucas J, Prevot LE. 1991.** Phosphates and fossil preservation. In: Allison P, Briggs D,
783 eds. *Taphonomy, Releasing the Data Locked in the Fossil Record*. Plenum Press: New
784 York. 389-409
- 785 **Lukeneder A, Surmik D, Gorzelak P, Niedźwiedzki R, Brachaniec T, Salamon MA. 2020.**
786 Bromalites from the Upper Triassic Polzberg section (Austria); insights into trophic
787 interactions and food chains of the Polzberg palaeobiota. *Scientific Reports* **10**:20545 DOI
788 10.1038/s41598-020-77017-x.
- 789 **Musiał T. 1987.** Miocen Roztocza (Polska południowo-wschodnia). *Prace Państwowego*
790 *Instytutu Geologicznego* **31**:5-149
- 791 **Mustoe GE. 2001.** Enigmatic origin of ferruginous coprolites: evidence from the Miocene
792 Wilkes formation, Southwestern Washington. *GSA Bulletin* **113**:673-681 DOI
793 10.1130/0016-7606(2001)113<0673:EOOFCE>2.0.CO;2.
- 794 **Niedźwiedzki G, Bajdek P, Owocki K, Kear BP. 2016.** An Early Triassic polar predator
795 ecosystem revealed by vertebrate coprolites from the Bulgo Sandstone (Sydney Basin) of
796 southeastern Australia. *Palaeogeography, Palaeoclimatology, Palaeoecology* **464**:5-15
797 DOI 10.1016/j.palaeo.2016.04.003.

- 798 **Olchowy P, Krajewski M, Felisiak I. 2019.** Late Jurassic facies succession of the Kleszczów
799 Graben area (southern border of the Łódź Depression, peri-Tethyan shelf, central Poland).
800 *Geological Quarterly* **63**:657-681 DOI 10.7306/gq.1496.
- 801 **Peñalver E, Gaudant J. 2010.** Limnic food web and salinity of the Upper Miocene Bicorn
802 palaeolake (eastern Spain). *Palaeogeography, Palaeoclimatology, Palaeoecology* **297**:683-
803 696 DOI 10.1016/j.palaeo.2010.09.017.
- 804 **Pesquero DM, Salesa JM, Espílez E, Mampel L, Siliceo G, Alcalá L. 2011.** An exceptionally
805 rich hyaena coprolites concentration in the Late Miocene mammal fossil site of La Roma 2
806 (Teruel, Spain): taphonomical and palaeoenvironmental inferences. *Palaeogeography,*
807 *Palaeoclimatology, Palaeoecology* **311**:30-37 DOI 10.1016/j.palaeo.2011.07.013.
- 808 **Peterson CD, Madin IP. 1997.** Coseismic paleoliquefaction in the central Cascadia margin
809 USA. *Oregon Geology* **59**:51-74
- 810 **Popov SV, Akhmetiev MA, Burgova EM, Lopatin AV, Amitrov OV, Andreyeva-**
811 **Grigorovich AS, Zaporozhec NI, Zherikhin VV, Krasheninnikov VA,**
812 **Nikolaeva IA, Sytchevskaya EK, Scherba IB. 2002.** Biogeography of the
813 Northern Peri-Tethys from the Late Eocene to the Early Miocene, part 2: Early
814 Oligocene. *Paleontological Journal* **36 (Suppl. 3)**:S185-S259
- 815 **Qvarnström M, Wernström JV, Wawrzyniak Z, Barbacka M, Pacyna G, Górecki A, Ziaja**
816 **J, Jarzynka A, Owocki K, Sulej T, Marynowski L, Pieńkowski G, Ahlberg PE,**
817 **Niedźwiedzki G. 2024.** Digestive contents and food webs record the advent of dinosaur
818 supremacy. *Nature* **636**:397-403 DOI 10.1038/s41586-024-08265-4.
- 819 **Qvarnström M, Anagnostakis S, Lindskog A, Scheer U, Vajda V, Rasmussen BW,**
820 **Lindgren J, Eriksson ME. 2019.** Multi-proxy analyses of Late Cretaceous coprolites
821 from Germany. *Lethaia* **52**:550-569 DOI 10.1111/let.12330.
- 822 **Richter G, Baszio S. 2001.** Traces of a limnic food web in the Eocene Lake Messel – a
823 preliminary report based on fish coprolite analyses. *Palaeogeography, Palaeoclimatology,*
824 *Palaeoecology* **166**:345-368 DOI 10.1016/S0031-0182(00)00218-2.
- 825 **Richter G, Wedmann S. 2005.** Ecology of the Eocene Lake Messel revealed by analysis
826 of small fish coprolites and sediments from a drilling core. *Palaeogeography,*
827 *Palaeoclimatology, Palaeoecology* **223**:147-161 DOI 10.1016/j.palaeo.2005.04.002.
- 828 **Roberts AE. 1958.** *Geology and coal resources of the Toledo-Castle Rock District, Cowlitz and*
829 *Lewis Counties.* Washington, D.C.: U.S. Geological Survey Bulletin.
- 830 **Román Z, Segesdi M, Sebe K, Földes T, Bakrač K, Virág A, Botfalvai G. 2024.**
831 Palaeontological and taphonomical investigations of the exceptionally rich concentration of
832 Miocene vertebrate coprolites from Pécs-Danitzpuszta (Hungary, Mecsek Mts.). *Historical*
833 *Biology* **37**:663-678 DOI 10.1080/08912963.2024.2324435.
- 834 **Rummy P, Halaçlar K, Chen H. 2021.** The first record of exceptionally-preserved spiral
835 coprolites from the Tsagan-Tsab formation (Lower Cretaceous), Tatal, western Mongolia.
836 *Scientific Reports* **11**:7891 DOI 10.1038/s41598-021-87090-5.

- 837 **Salamon MA, Niedźwiedzki R, Gorzelak P, Lach R, Surmik D. 2012.** Bromalites from the
838 Middle Triassic of Poland and the rise of the Mesozoic Marine Revolution.
839 *Palaeogeography, Palaeoclimatology, Palaeoecology* **321-322**:142-150 DOI
840 10.1016/j.palaeo.2012.01.029.
- 841 **Salamon MA, Radwańska U, Paszcza K, Krajewski M, Brachaniec T, Niedźwiedzki R,**
842 **Gorzelak P. 2024.** The latest shallow-sea isocrinids from the Miocene of Paratethys and
843 implications to the Mesozoic marine revolution. *Scientific Reports* **14**: 17932 DOI
844 10.1038/s41598-024-67687-2.
- 845 **Schweigert G, Dietl G. 2012.** Vertebrate coprolites from the Nusplingen Lithographic
846 Limestone (Upper Jurassic, SW Germany). *New Mexico Museum of Natural History &*
847 *Science Bulletin* **57**:215-220
- 848 **Schwimmer DR, Weems RE, Sanders AE. 2015.** A Late Cretaceous shark coprolite
849 with baby freshwater turtle vertebrae inclusions. *Palaios* **30**:707-713 DOI
850 10.2110/palo.2015.019.
- 851 **Segesdi M., Botfalvai G, Bodor ER, Ósi A, Buczkó K, Dallos Z, Tokai R, Földes T. 2017.**
852 First report on vertebrate coprolites from the Upper Cretaceous (Santonian) Csehbánya
853 Formation of Iharkút, Hungary. *Cretaceous Research* **74**:87-99 DOI
854 10.1016/j.cretres.2017.02.010.
- 855 **Seilacher A, Marshall C, Skinner WC, Tsuihiji T. 2001.** A fresh look at sideritic coprolites.
856 *Paleobiology* **27**:7-13 DOI 10.1666/0094-8373(2001)027<0007:aflasc>2.0.co;2.
- 857 **Spencer PK. 1993.** The “coprolites” that aren't: the straight poop on specimens from the
858 Miocene of Southwestern Washington State, Ichnos. *An International Journal for Plant*
859 *and Animal Traces* **2**:231-236
- 860 **Spencer PK. 1997.** The method of multiple working hypotheses in undergraduate education with
861 an example of its application and misapplication. *Journal of Geoscience Education* **45**:123-
862 128
- 863 **Spencer PK, Tuttle FH. 1980.** Coprolites or pseudo-coprolites? New evidence concerning
864 the origin of Washington coprolites. *Geological Society of America* **12**:153
- 865 **Stringer GL, King L. 2012.** Late Eocene shark coprolites from the Yazoo Clay in northern
866 Louisiana. *New Mexico Museum of Natural History & Science Bulletin* **57**:275-310
- 867 **Studencki W. 1999.** Red-algal limestones in the Middle Miocene of the Carpathian Foredeep in
868 Poland: facies variability and palaeoclimatic implications. *Geological Quarterly* **43**:395-
869 404
- 870 **Stworzewicz E. 1999.** Miocene Land Snails From Bełchatów (Central Poland). Pupilloidea
871 (Gastropoda Pulmonata). Systematic, Biostratigraphic And Palaeoecological Studies. *Folia*
872 *Malacologica* **7**:133-170 DOI 10.12657/folmal.007.015.
- 873 **Świdnicka E. 2007.** *Aturia* sp. (Nautiloidea) from Oligocene of the Menilite-Krosno Series
874 of the Polish Carpathians. In: Żylińska A, ed. *Granice Paleontologii*. Materiały XX
875 konferencji Naukowej Paleobiologów i Biostratygrafów PTG: Warszawa. 137-138
- 876 **Tolar T, Galik A. 2019.** A Study of Dog Coprolite from Late Neolithic Pile-Dwelling Site in
877 Slovenia. *Archaeological Discovery* **7**:20-29 DOI 10.4236/ad.2019.71002.

- 878 **Tomassini LR, Montalvo IC, Bargo MS, Vizcaíno FS, Cuitiño IJ. 2019.** Sparassodonta
879 (Metatheria) coprolites from the early-mid Miocene (Santacrucian age) of Patagonia
880 (Argentina) with evidence of exploitation by coprophagous insects. *Palaios* **34**:639-651
881 DOI 10.2110/palo.2019.080.
- 882 **Vajda V, Fernández MDP, Villanueva-Amadoz U, Lehsten V, Alcalá L. 2016.** Dietary and
883 environmental implications of Early Cretaceous predatory dinosaur coprolites from Teruel,
884 Spain. *Palaeogeography, Palaeoclimatology, Palaeoecology* **464**:134-142 DOI
885 10.1016/j.palaeo.2016.02.036.
- 886 **Wang X, White SC, Balisi M, Biewer J, Sankey J, Garber D, Tseng ZJ. 2018.** First
887 bone-cracking dog coprolites provide new insight into bone consumption in
888 *Borophagus* and their unique ecological niche. *eLife* **7**:e34773 DOI 10.7554/eLife.34773.
- 889 **Wetmore A. 1943.** The occurrence of feather impressions in the Miocene deposits of Maryland.
890 *The Auk* **60**:440-441
- 891 **Widera M, Kłeszk J, Urbański P. 2024.** The geology of the deepest Cenozoic lignite-rich
892 grabens in Poland with particular reference to their lithostratigraphy: a comparative study.
893 *Geology, Geophysics & Environment* **50**:131-143 DOI 10.7494/geol.2024.50.2.131.
- 894 **Wilson MVH. 1987.** Predation as a source of fish fossils in Eocene lake sediment.
895 *Palaios* **2**:497-504 DOI 10.2307/3514620.
- 896 **Wood JR, Wilmskrust J. 2014.** Late Quaternary terrestrial vertebrate coprolites from New
897 Zealand. *Quaternary Science Reviews* **98**:33-34 DOI 10.1016/j.quascirev.2014.05.020.
- 898 **Wood JR, Wilmskrust J. 2016.** A protocol for subsampling Late Quaternary coprolites for
899 multi-proxy analysis. *Quaternary Science Reviews* **138**:1-5 DOI
900 10.1016/j.quascirev.2016.02.018.
- 901 **Wysocka A, Jasionowski M, Peryt TM. 2007.** Miocen Roztocza. Miocene of the Roztocze
902 Hills. *Biuletyn Państwowego Instytutu Geologicznego* **422**:79-96
- 903 **Zatoń M, Niedźwiedzki G, Marynowski L, Benzerara K, Pott C, Cosmidis J, Krzykawski
904 T, Filipiak P. 2015.** Coprolites of Late Triassic carnivorous vertebrates from Poland: an
905 integrative approach. *Palaeogeography, Palaeoclimatology, Palaeoecology* **430**:21-46
906 DOI 10.1016/j.palaeo.2015.04.009.

907

908 **Figures captions**

909

910 **Figure 1. Geological settings of studied locations. (A).** Map of Poland with marked research
911 areas. **(B).** Kleszczów Graben area. **(C).** Southern edge of the Holy Cross Mountains. **(D).** Turów
912 area. **(E).** Roztocze. **(F).** Menilite-Krosno Series of the Outer Carpathians. **(G).** Stratigraphic
913 section and positions of sites where the coprolites have been documented. Compiled and slightly
914 modified after: *Kotlarczyk et al., 2006; Wysocka, Jasionowski & Peryt, 2007; Olchowy,*
915 *Krajewski & Felisiak, 2019; Brachaniec et al., 2022; Salamon et al., 2024.*

916

917 **Figure 2. Examples of coprolites collected in the Oligocene and Miocene marine sediments**
918 **of Poland.** Kąkolówka I:(A) GIUS 10–3796/O/2; (B) GIUS 10–3796/O/7; (C) GIUS 10–



919 3796/O/23; Kąkolówka II: (D) GIUS 10–3796/O/154; (E) GIUS 10–3796/O/181; (F) Kąkolówka
 920 I, GIUS 10–3796/O/60; (G) Kąkolówka I, GIUS 10–3796/O/77; Wola Czudecka: (H) GIUS 10–
 921 3796/O/251; (I) GIUS 10–3796/O/253; (J) GIUS 10–3796/O/259; (K) GIUS 10–3796/O/274;
 922 (L) Futoma, GIUS 10–3796/O/279; (M) Futoma, GIUS 10–3796/O/282; Kąkolówka I: (N)
 923 GIUS 10–3796/O/96; (O) GIUS 10–3796/O/98; (P) GIUS 10–3796/O/107; (R) GIUS 10–
 924 3796/O/111; (S) GIUS 10–3796/O/135; (T) Jamna Dolna, GIUS 10–3796/O/294; (U) Kąkolówka
 925 I, GIUS 10–3796/O/139. Scale bars 5 mm.

926

927 **Figure 3. Examples of coprolites collected in Oligocene and Miocene marine. (A–D) and**
 928 **non-marine (E–N) sediments of Poland. Równe: (A) GIUS 10–3796/O/297; Jasienica Rosielna**
 929 **(B) GIUS 10–3796/O/299; Kąkolówka I (C) GIUS 10–3796/O/144; Temeszów (D) GIUS 10–**
 930 **3796/M/33; Gochulów (E) GIUS 10–3796/M/13; Roztocze area-Żelebsko (F) GIUS 10–**
 931 **3796/M/32; Turów area (G) GIUS 10–3796/M/16; (H) GIUS 10–3796/M/19; (I) GIUS 10–**
 932 **3796/M/23; (J) GIUS 10–3796/M/28; (K) GIUS 10–3796/M/30; Bełchatów (L) GIUS 10–**
 933 **3796/M/2; (M) GIUS 10–3796/M/6; (N) GIUS 10–3796/M/11. Scale bars 5 mm.**

934

935 **Figure 4. BSE images of investigated coprolites from Oligocene coprolites of the Menilite-**
 936 **Krosno Series of the Outer Carpathians. (A–E, J) Fish bones. (F–I?) Scales. (K–L) Teeth. (A–**
 937 **B, D, E, G–I) Kąkolówka I locality, GIUS 10–3796/O/107; (C) Jasienica Rosielna locality,**
 938 **GIUS 10–3796/O/300; (F, J–L) Jamna Dolna locality, GIUS 10–3796/O/294. Scale bars 30 um.**

939

940 **Figure 5. BSE images showing unidentified fossil bone remains embedded within coprolite**
 941 **matrix from Miocene of the Menilite-Krosno Series of the Outer Carpathians (GIUS 10–**
 942 **3796/M/33 and 34 respectively). (A) The coprolite/matrix boundary and the surrounding**
 943 **sediment, with bone fragments visible in both. (B) Remains of different morphology. (C–E)**
 944 **Close-ups of selected fossilized fragments. Scale bars 200 um.**

945

946 **Figure 6. Recent faeces. (A) Brown hare (*Lepus europeus*). (B) European mole (*Talpa***
 947 ***europaea*). (C) Guinea pig (*Cavia porcellus*). (D) Swinhoe's striped squirrel (*Tamias swinhoei*).**
 948 **(E) Seba's short-tailed bat (*Carollia perspicillata*). (F) House sparrow (*Passer domesticus*). (G)**
 949 **Syngnathidae. (H) City pigeon (*Columba livia forma urbana*). (I) Zebra moray (*Gymnomuraena***
 950 ***zebra*). (J) Hermit crab (*Coenobita brevipanum*). (K) Flying crab (*Liocarcinus holsatus*). (L)**
 951 **Sea cucumber (*Holothuria* sp.; redrawn from *Knaust & Hoffmann, 2020*). (M) Cephalopod**
 952 **(*Nautilus pompilius*; redrawn from *Knaust & Hoffmann, 2020*). (N) Perciformes. Scale bars 1**
 953 **cm.**

954

955 **Figure 7. Examples of crab fossils representing *Liocarcinus oligocenicus* from the Oligocene**
 956 **marine strata of the Menilite-Krosno Series (The Outer Carpathians, Poland). (A) Kr.J-7.**
 957 **(B) Kr.H-1. (C) Kr.JR-2. (D) Kr.J-3. (E) Kr.J-11. (F) Kr.J-16. (G) Kr.J-12. (H) Kr.J-6. (I) Kr.J-**
 958 **3. Scale bar equals 1 cm.**

959



960 **Figure 8. Examples of fossil fish from the Oligocene marine strata of ofthe Menilite-Krosno**
961 **Series (The Outer Carpathians, Poland). (A)** Specimen representing unidentified taxa, Ma 31.
962 **(B)** *Clupea* sp., ROJ-215. **(C)** Specimen representing unidentified taxa,ROJ-212. **(D)** Specimen
963 representing unidentified taxa, ROL-305. **(E)** Specimen representing unidentified taxa, ROJ-307.
964 **(F)** *Eomyctophum* sp., Ma-52. **(G)** *Holosteus* sp., ROJR-170. **(H)** Unidentified taxa of
965 Scombridae family, ROL-47. **(I)** *Centriscus* sp., ROJ-514. **(J)** *Argyropelecus* sp., ROL-221. **(K)**
966 *Hipposyngnathus* sp., ROJ-211. **(L)** Specimen representing unidentified taxa, ROL-328. Scale
967 bar equals 1 cm.

968

969 **Figure 9. Examples of fossil fish from the Oligocene marine strata of the Menilite-Krosno**
970 **Series (The Outer Carpathians, Poland). (A)** *Holosteus* sp., ROJ-17. **(B)** *Holosteus* sp., ROJ-
971 22. **(C)** *Holosteus* sp., ROJ-45. **(D)** *Oligoserranoides* sp., ROR-153. **(E)** *Oligoserranoides* sp.,
972 ROJ-47. **(F)** *Oligoserranoides* sp., RORR-7. Scale bar equals 1 cm.

973

974 **Figure 10. Examples of fossil fish collected in Oligocene marine strata ofthe Menilite-**
975 **Krosno Series (The Outer Carpathians, Poland). (A)** *Scopeloides* sp. GIUS10–3796/O/F1. **(B)**
976 Jaw of *Lepidopus* sp. **(C, D)** probably *Scopeloides* sp. GIUS10–3796/O/F3, 4. Scale bar equals 1
977 cm.

978

979 **Figure 11. Examples of fossil fish from the Oligocene marine strata ofthe Menilite-Krosno**
980 **Series (The Outer Carpathians, Poland). (A)** *Lepidopus* sp., ROU-400. **(B)** *Lepidopus* sp.,
981 ROU-405. **(C)** *Lepidopus* sp., Ma-5. **(D)** *Lepidopus* sp., ROU-40. **(E)** *Lepidopus* sp., ROU-42.
982 **(F)** *Lepidopus* sp., ROL-55. **(G)** *Isurus* sp., ROM-ZR-100.**(H)** *Isurus* sp., ROM-ZR-103. **(I)**
983 *Isurus* sp., ROM-ZR-107. **(J)** *Isurus* sp., ROM-ZR-112. **(K)** *Isurus* sp., ROJ-ZR-123. Scale bar
984 equals 1 cm.

985

986 **Figure 12. Examples of feathers representing unidentified taxa from the Oligocene marine**
987 **strata of the Menilite-Krosno Series (The Outer Carpathians, Poland). (A)** MSMD.Av. Jam-
988 11. **(B)** MSMD.Av. Jam-14. **(C)** MSMD.Av. S.Bir-3. **(D)** MSMD.Av. Jam-1. **(E)** MSMD.Av.
989 J.Ros-9. **(F)** MSMD.Av. Jam-15. Scale bar equals 1 cm.

990

991 **Figure 13. Some examples of vertebrate remains documented in Miocenian deposits of the**
992 **Kleszczów Graben, central Poland. Acronyme number: GIUS 10–3796V. (A)** Jaw of a
993 Lacertidae lizard. **(B)** Otolith of *Klingobius andjelkocae*. **(C, D)** Vertebrae of indeterminated
994 rodents. **(E–H)** Bones of indeterminate vertebrates. **(I)** Jaw of a rodent. **(J)** Tooth of Chiroptera.
995 **(K)** Incisor of Castocrinae. **(L–N)** Talpidaeteeth. **(O)** Tooth of an unidentified predator. Scale bar
996 equals 1 mm.

997

998

Figure 1

Geological settings of studied locations.

(A). Map of Poland with marked research areas. (B). Kleszczów Graben area. (C). Southern edge of the Holy Cross Mountains. (D). Turów area. (E). Roztocze. (F). Menilite-Krosno Series of the Outer Carpathians. (G). Stratigraphic section and positions of sites where the coprolites have been documented. Compiled and slightly modified after: *Kotlarczyk et al., 2006; Wysocka, Jasionowski & Peryt, 2007; Olchoway, Krajewski & Felisiak, 2019; Brachaniec et al., 2022; Salamon et al., 2024.*

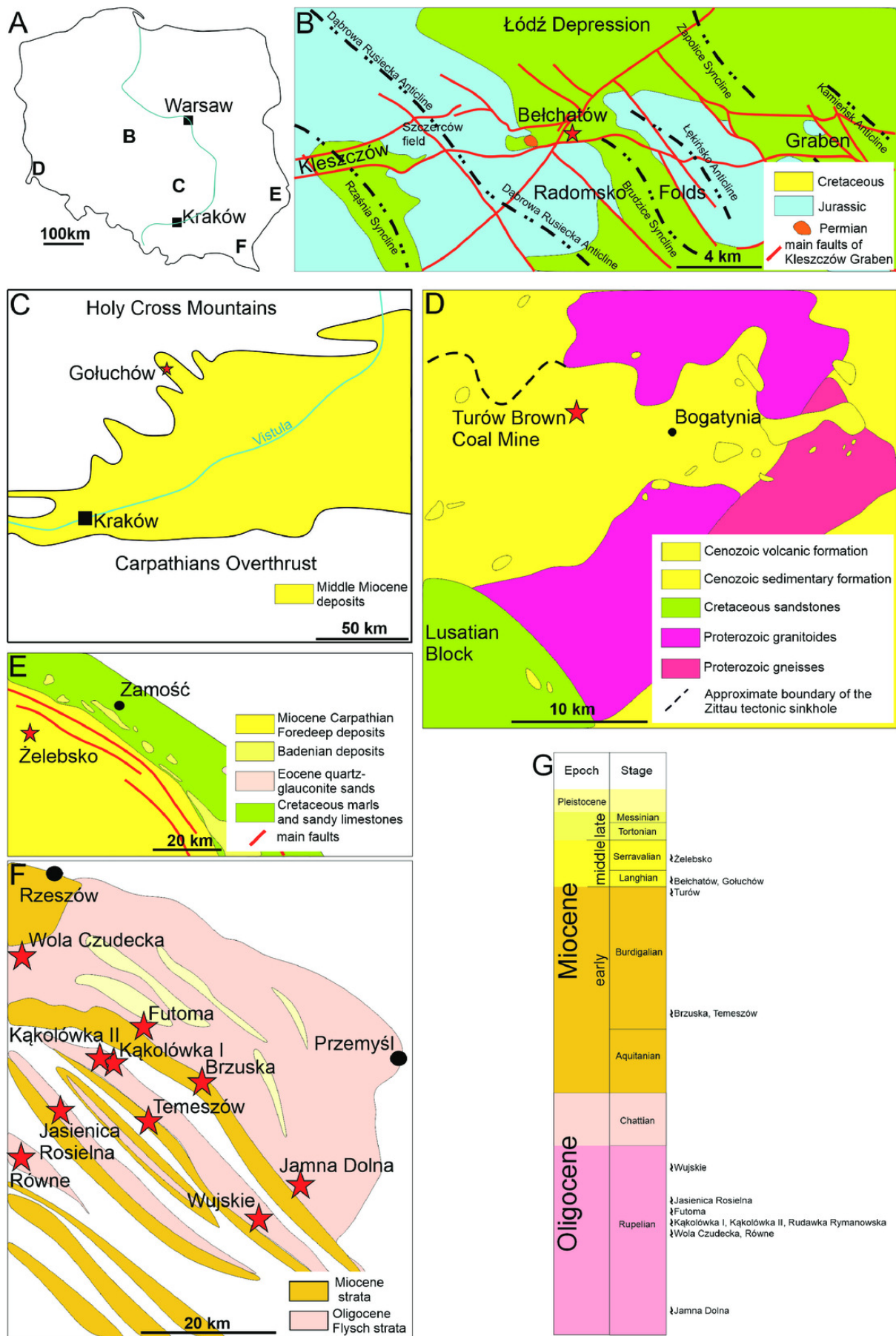


Figure 2

Examples of coprolites collected in the Oligocene and Miocene marine sediments of Poland.

Kąkolówka I: (A) GIUS 10-3796/O/2; (B) GIUS 10-3796/O/7; (C) GIUS 10-3796/O/23;
Kąkolówka II: (D) GIUS 10-3796/O/154; (E) GIUS 10-3796/O/181; (F) Kąkolówka I, GIUS
10-3796/O/60; (G) Kąkolówka I, GIUS 10-3796/O/77; Wola Czudecka: (H) GIUS
10-3796/O/251; (I) GIUS 10-3796/O/253; (J) GIUS 10-3796/O/259; (K) GIUS 10-3796/O/274;
(L) Futoma, GIUS 10-3796/O/279; (M) Futoma, GIUS 10-3796/O/282; Kąkolówka I: (N) GIUS
10-3796/O/96; (O) GIUS 10-3796/O/98; (P) GIUS 10-3796/O/107; (R) GIUS 10-3796/O/111;(S)
GIUS 10-3796/O/135; (T) Jamna Dolna, GIUS 10-3796/O/294; (U) Kąkolówka I, GIUS
10-3796/O/139. Scale bars 5 mm.

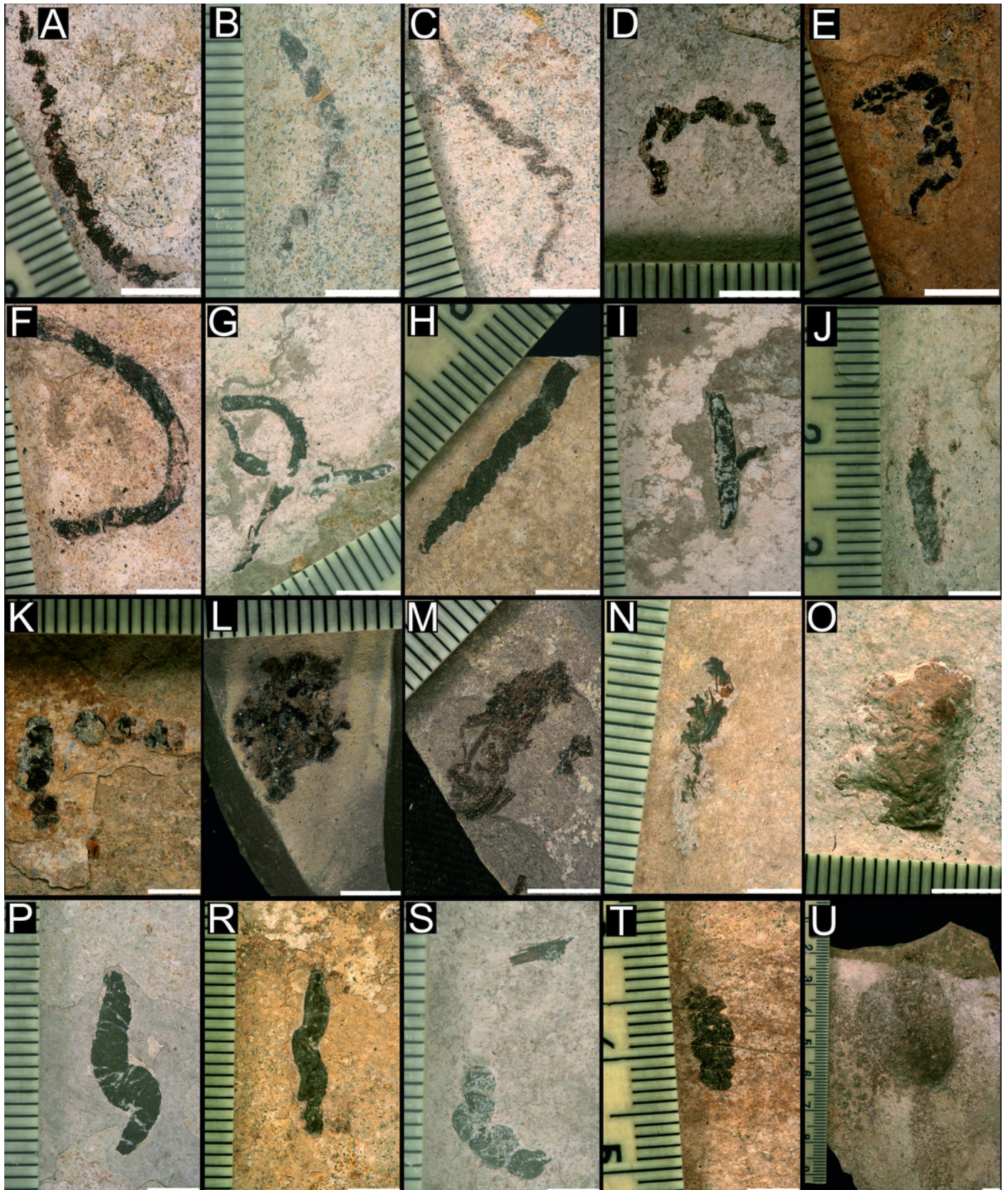


Figure 3

Examples of coprolites collected in Oligocene and Miocene marine.

(A-D) and non-marine (E-N) sediments of Poland. Równe: (A) GIUS 10-3796/O/297; Jasienica Rosielna (B) GIUS 10-3796/O/299; Kąkolówka I (C) GIUS 10-3796/O/144; Temeszów (D) GIUS 10-3796/M/33; Gochułów (E) GIUS 10-3796/M/13; Roztocze area-Żelebsko (F) GIUS 10-3796/M/32; Turów area (G) GIUS 10-3796/M/16; (H) GIUS 10-3796/M/19; (I) GIUS 10-3796/M/23; (J) GIUS 10-3796/M/28; (K) GIUS 10-3796/M/30; Bełchatów (L) GIUS 10-3796/M/2; (M) GIUS 10-3796/M/6; (N) GIUS 10-3796/M/11. Scale bars 5 mm.

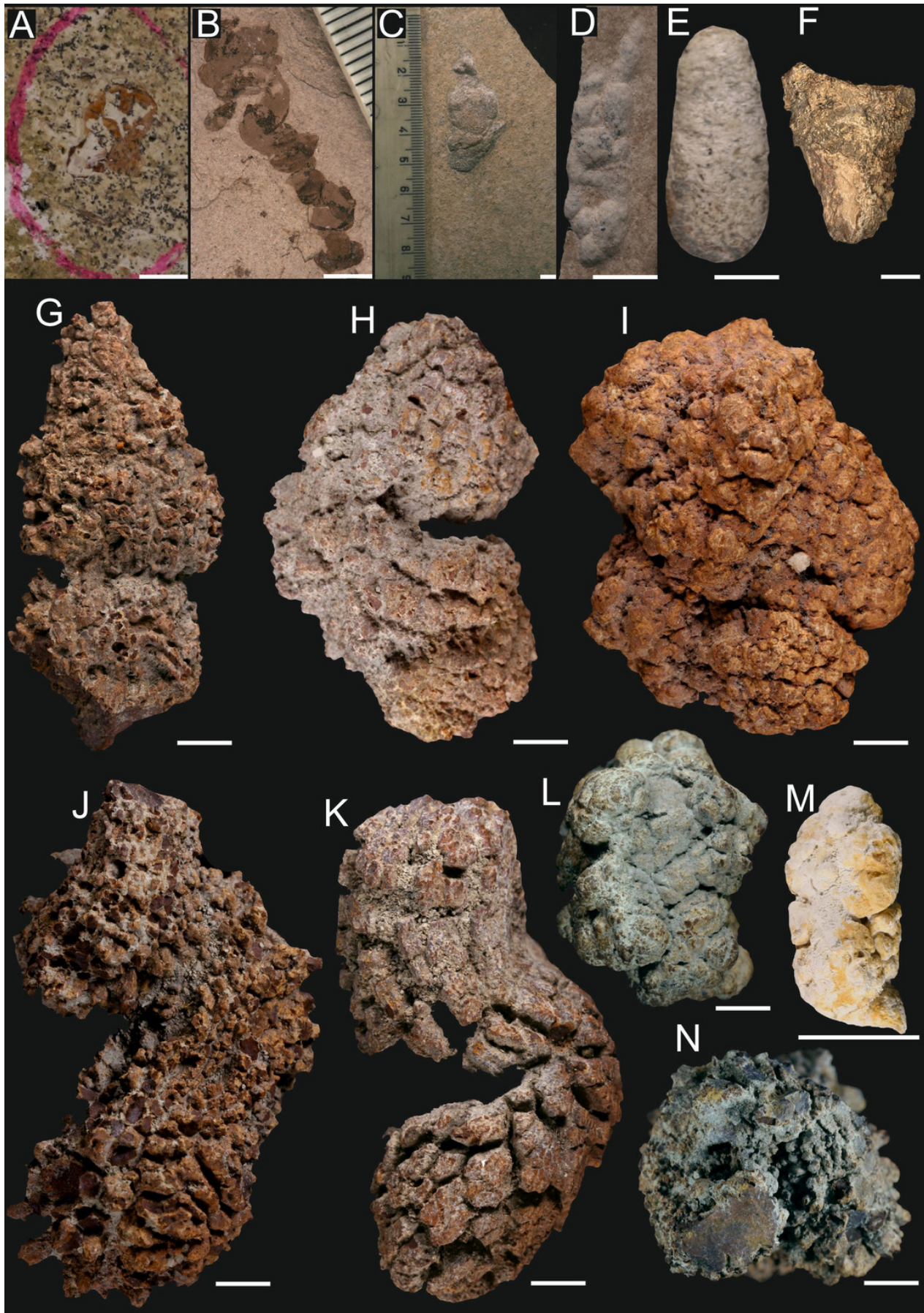


Figure 4

BSE images of investigated coprolites from Oligocene coprolites of the Menilite-Krosno Series of the Outer Carpathians.

(A - E, J) Fish bones. (F-I?) Scales. (K-L) Teeth. (A-B, D, E, G-I) Kąkolówka I locality, GIUS 10-3796/O/107; (C) Jasienica Rosielna locality, GIUS 10-3796/O/300; (F, J-L) Jamna Dolna locality, GIUS10-3796/O/294. Scale bars 30 μm .

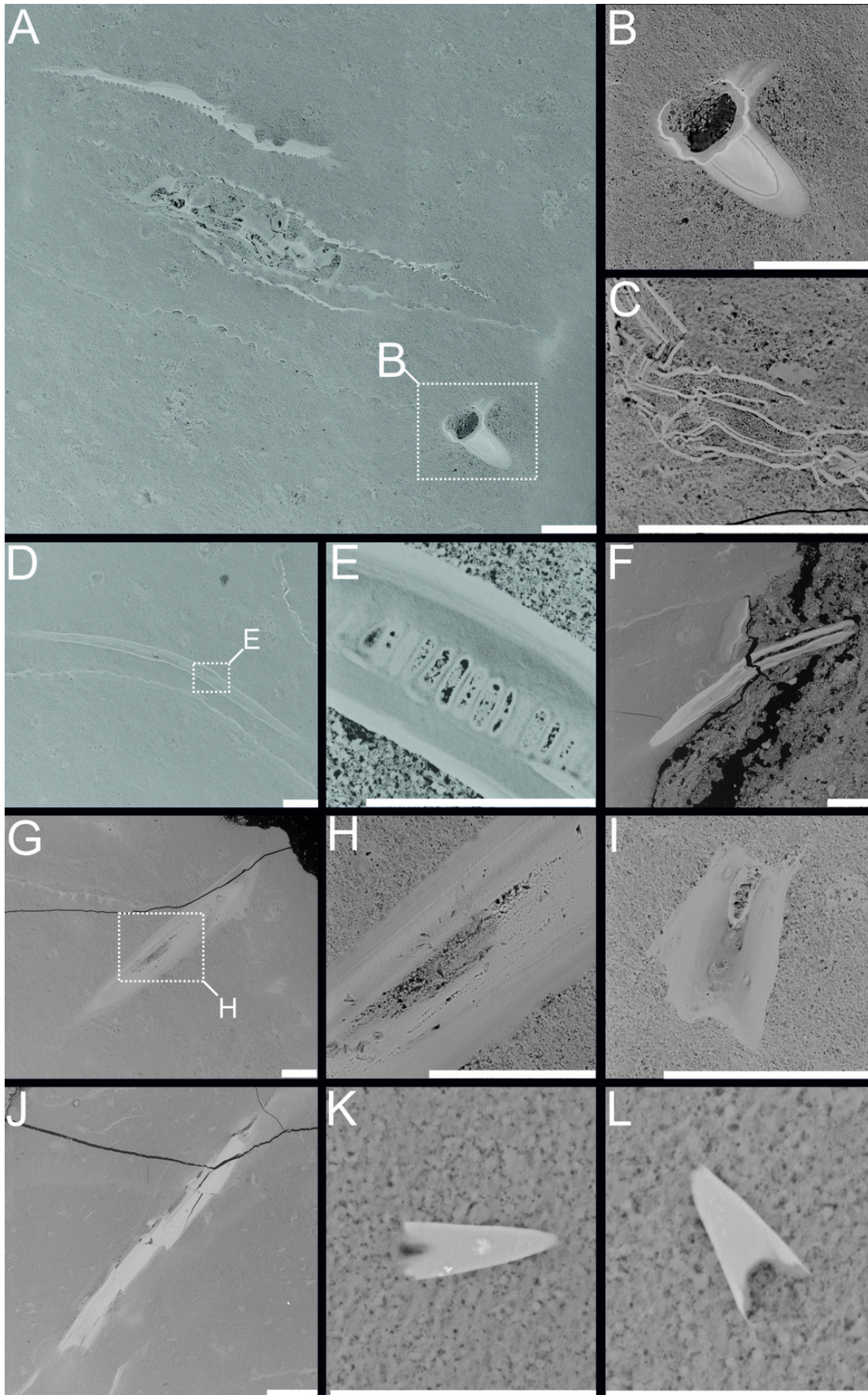


Figure 5

BSE images showing unidentified fossil bone remains embedded within coprolite matrix from Miocene of the Menilite-Krosno Series of the Outer Carpathians (GIUS 10-3796/M/33 and 34 respectively).

(A) The coprolite/matrix boundary and the surrounding sediment, with bone fragments visible in both. (B) Remains of different morphology. (C-E) Close-ups of selected fossilized fragments. Scale bars 200 μm .

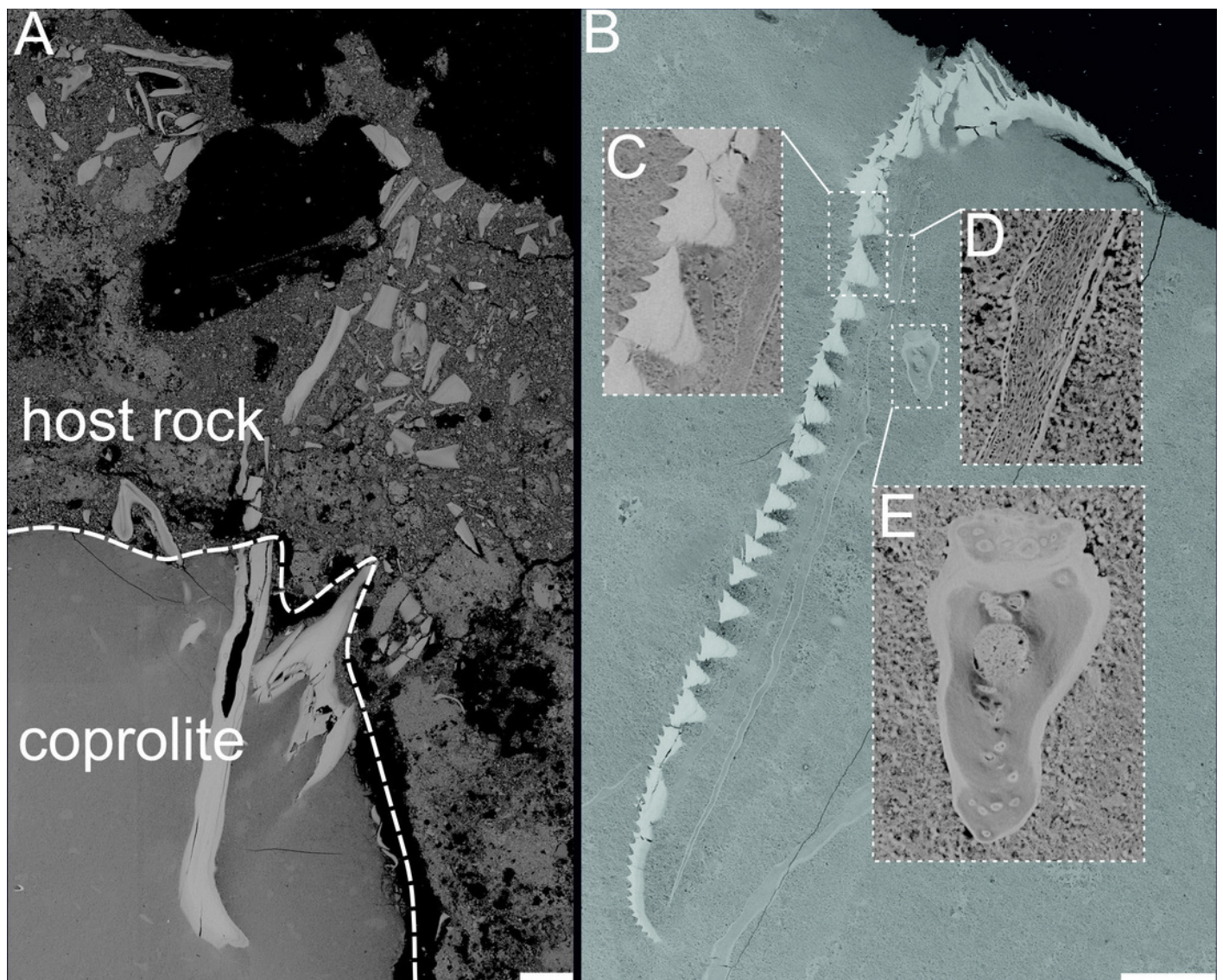


Figure 6

Recent faeces.

(A) Brown hare (*Lepus europeus*). (B) European mole (*Talpa europaea*). (C) Guinea pig (*Cavia porcellus*). (D) Swinhoe's striped squirrel (*Tamiops swinhoei*). (E) Seba's short-tailed bat (*Carollia perspicillata*). (F) House sparrow (*Passer domesticus*). (G) Syngnathidae. (H) City pigeon (*Columba livia forma urbana*). (I) Zebra moray (*Gymnomuraena zebra*). (J) Hermit crab (*Coenobita brevipanus*). (K) Flying crab (*Liocarcinus holsatus*). (L) Sea cucumber (*Holothuria* sp.; redrawn from *Knaust & Hoffmann, 2020*). (M) Cephalopod (*Nautilus pompilius*; redrawn from *Knaust & Hoffmann, 2020*). (N) Perciformes. Scale bars 1 cm.

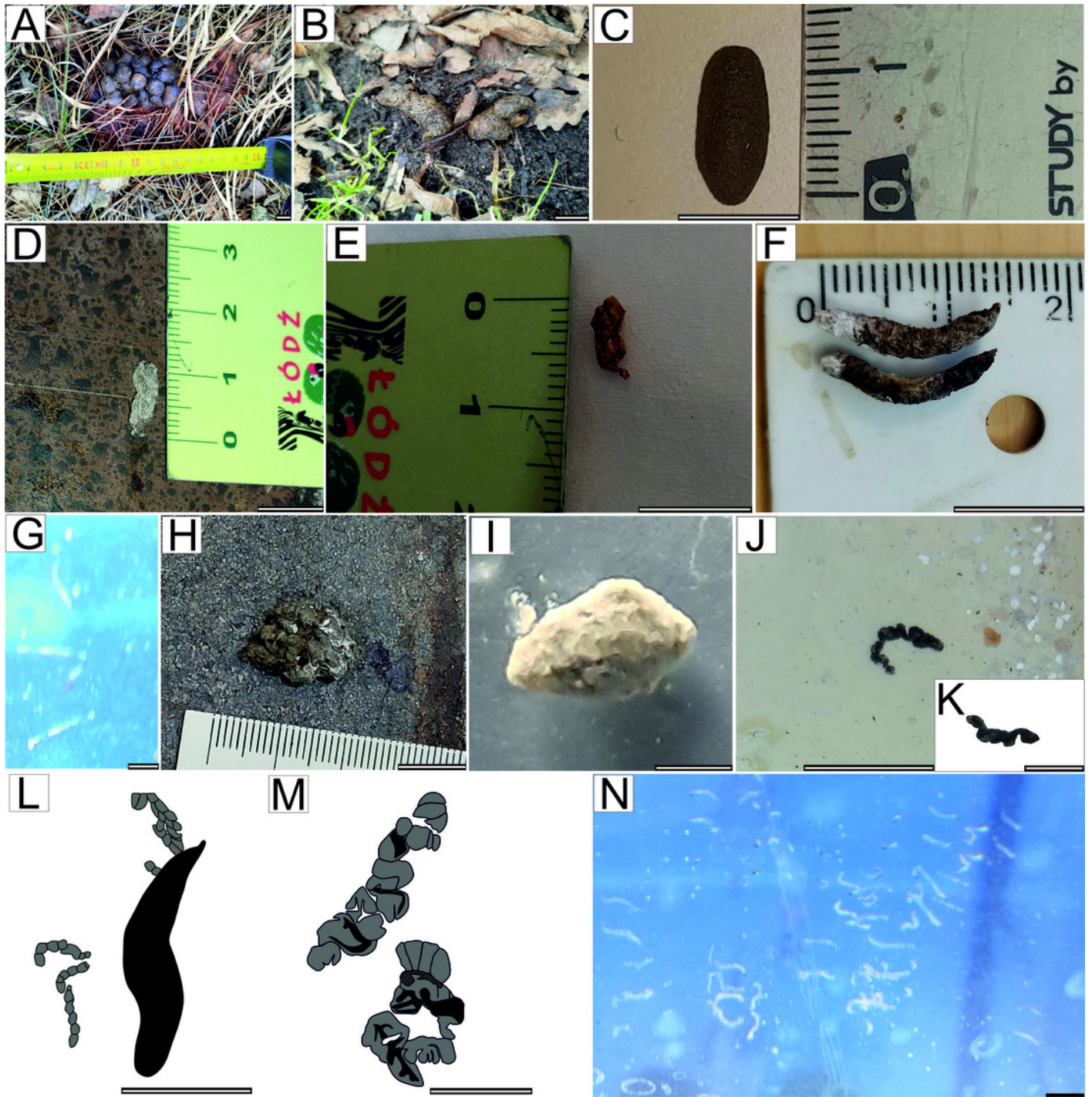


Figure 7

Examples of crab fossils representing *Liocarcinus oligocenicus* from the Oligocene marine strata of the Menilite-Krosno Series (The Outer Carpathians , Poland).

(A) Kr.J-7. (B) Kr.H-1. (C) Kr.JR-2. (D) Kr.J-3. (E) Kr.J-11. (F) Kr.J-16. (G) Kr.J-12. (H) Kr.J-6. (I) Kr.J-3. Scale bar equals 1 cm.

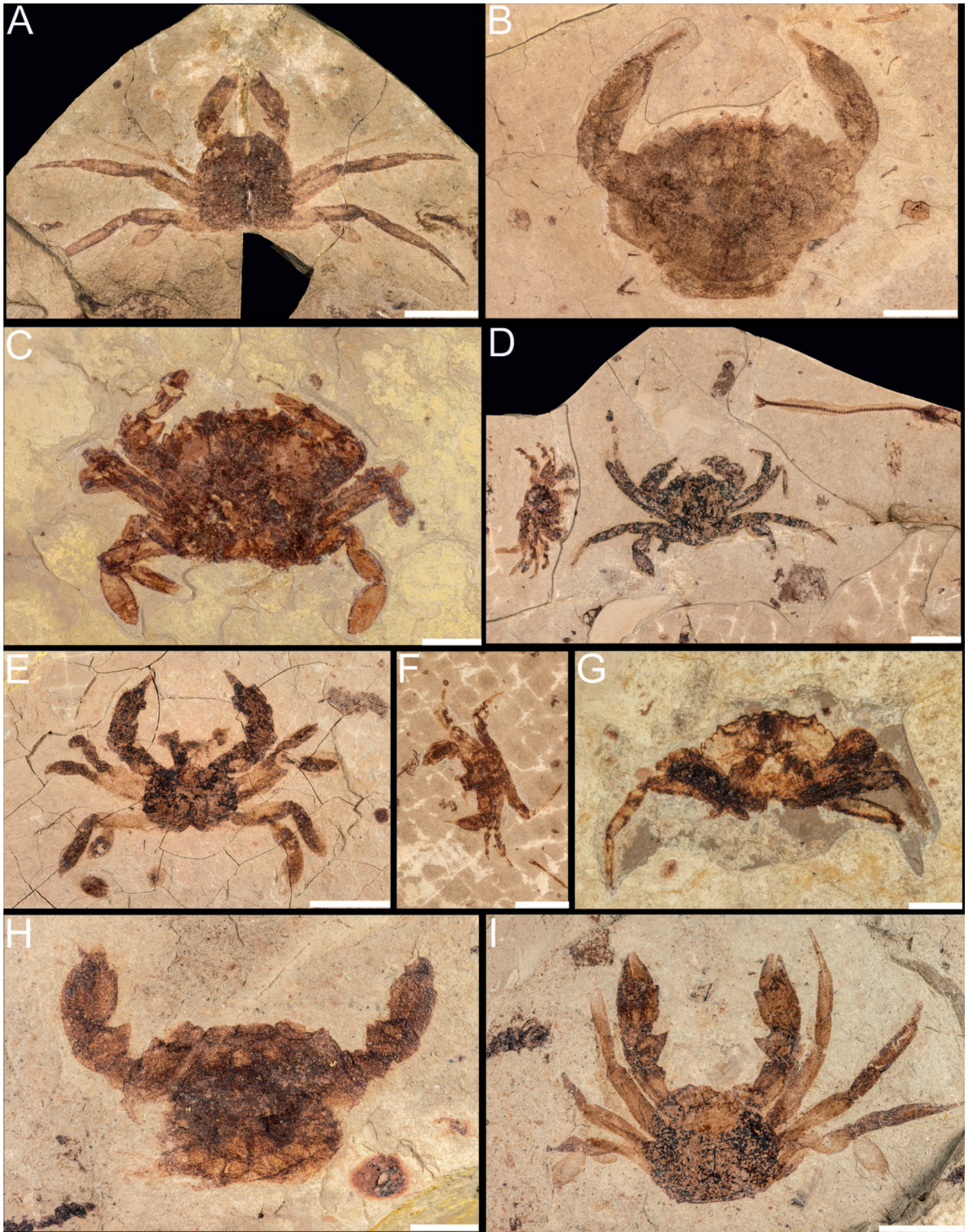


Figure 8

Examples of fossil fish from the Oligocene marine strata of the Menilite-Krosno Series (The Outer Carpathians, Poland).

(A) Specimen representing unidentified taxa, Ma 31. (B) *Clupea* sp., ROJ-215. (C) Specimen representing unidentified taxa, ROJ-212. (D) Specimen representing unidentified taxa, ROL-305. (E) Specimen representing unidentified taxa, ROJ-307. (F) *Eomyctophum* sp., Ma-52. (G) *Holosteus* sp., ROJR-170. (H) Unidentified taxa of Scombridae family, ROL-47. (I) *Centriscus* sp., ROJ-514. (J) *Argyropelecus* sp., ROL-221. (K) *Hipposyngnathus* sp., ROJ-211. (L) Specimen representing unidentified taxa, ROL-328. Scale bar equals 1 cm.

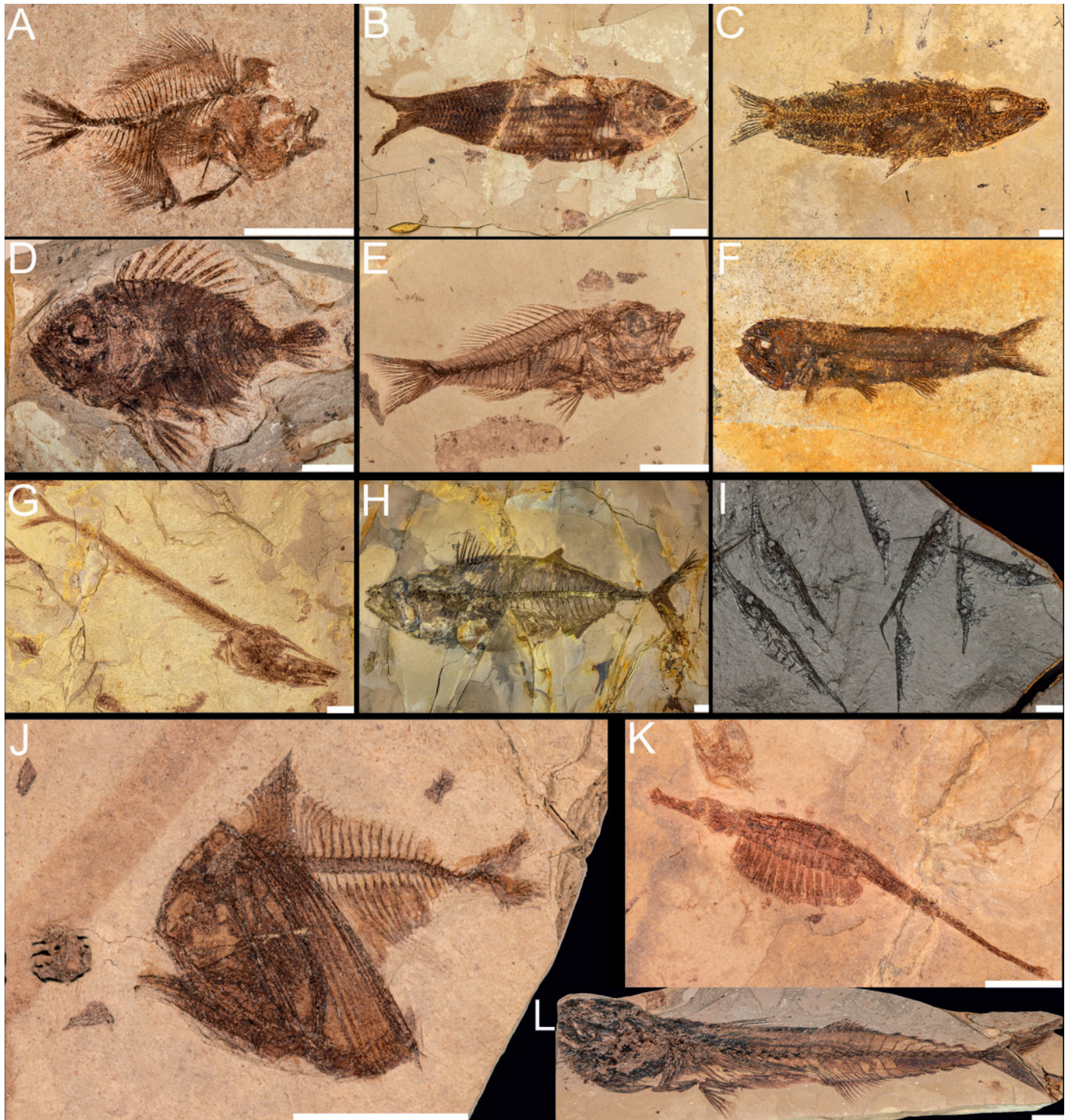


Figure 9

Examples of fossil fish from the Oligocene marine strata of the Menilite-Krosno Series (The Outer Carpathians, Poland).

(A) *Holosteus* sp., ROJ-17. (B) *Holosteus* sp., ROJ-22. (C) *Holosteus* sp., ROJ-45. (D) *Oligoserranoides* sp., ROR-153. (E) *Oligoserranoides* sp., ROJ-47. (F) *Oligoserranoides* sp., RORR-7. Scale bar equals 1 cm.

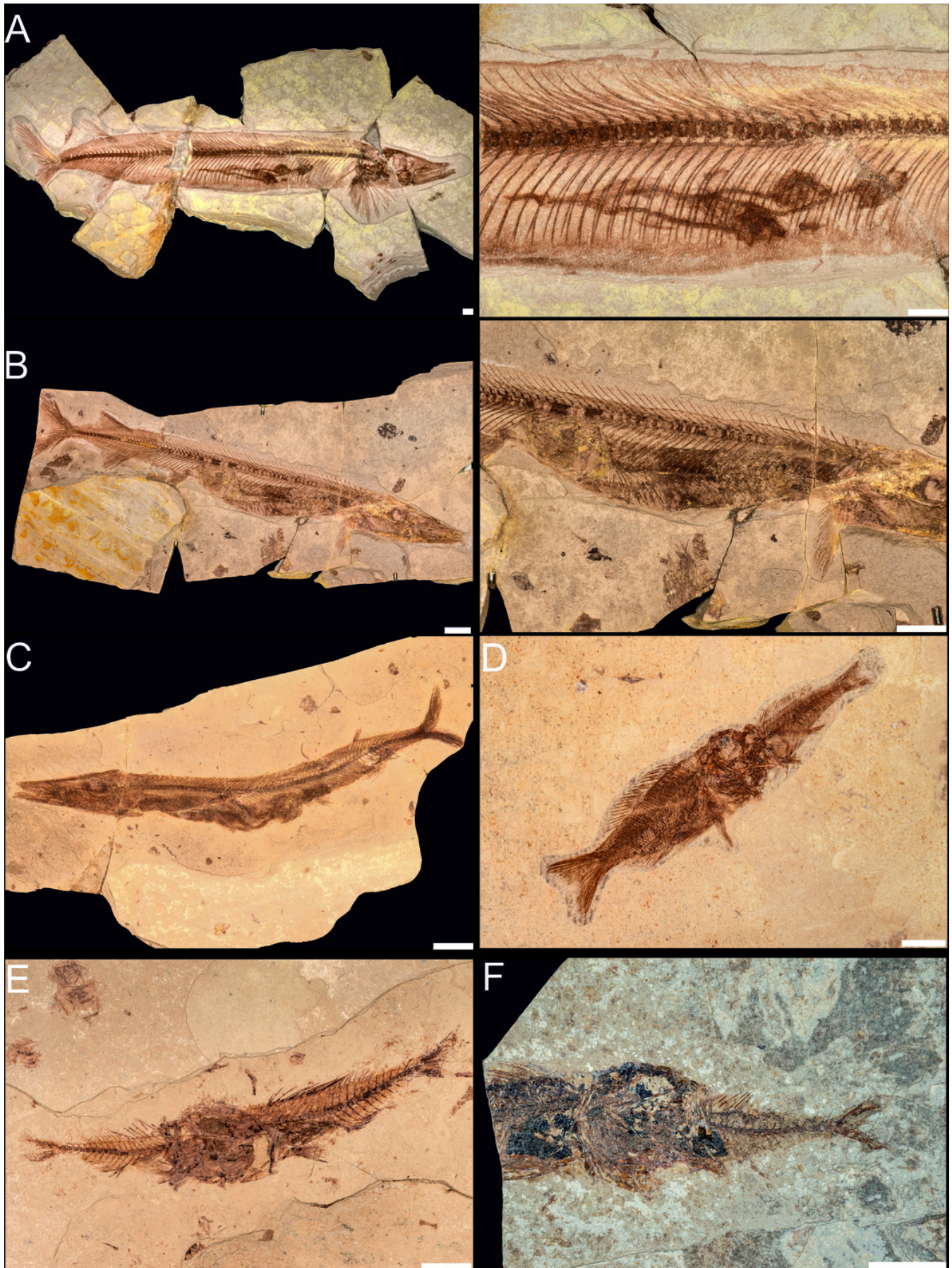


Figure 10

Examples of fossil fish collected in Oligocene marine strata of the Menilite-Krosno Series (The Outer Carpathians, Poland).

(A) *Scopeloides* sp. GIUS10-3796/O/F1. (B) Jaw of *Lepidopus* sp. (C, D) probably *Scopeloides* sp. GIUS10-3796/O/F3, 4. Scale bar equals 1 cm.

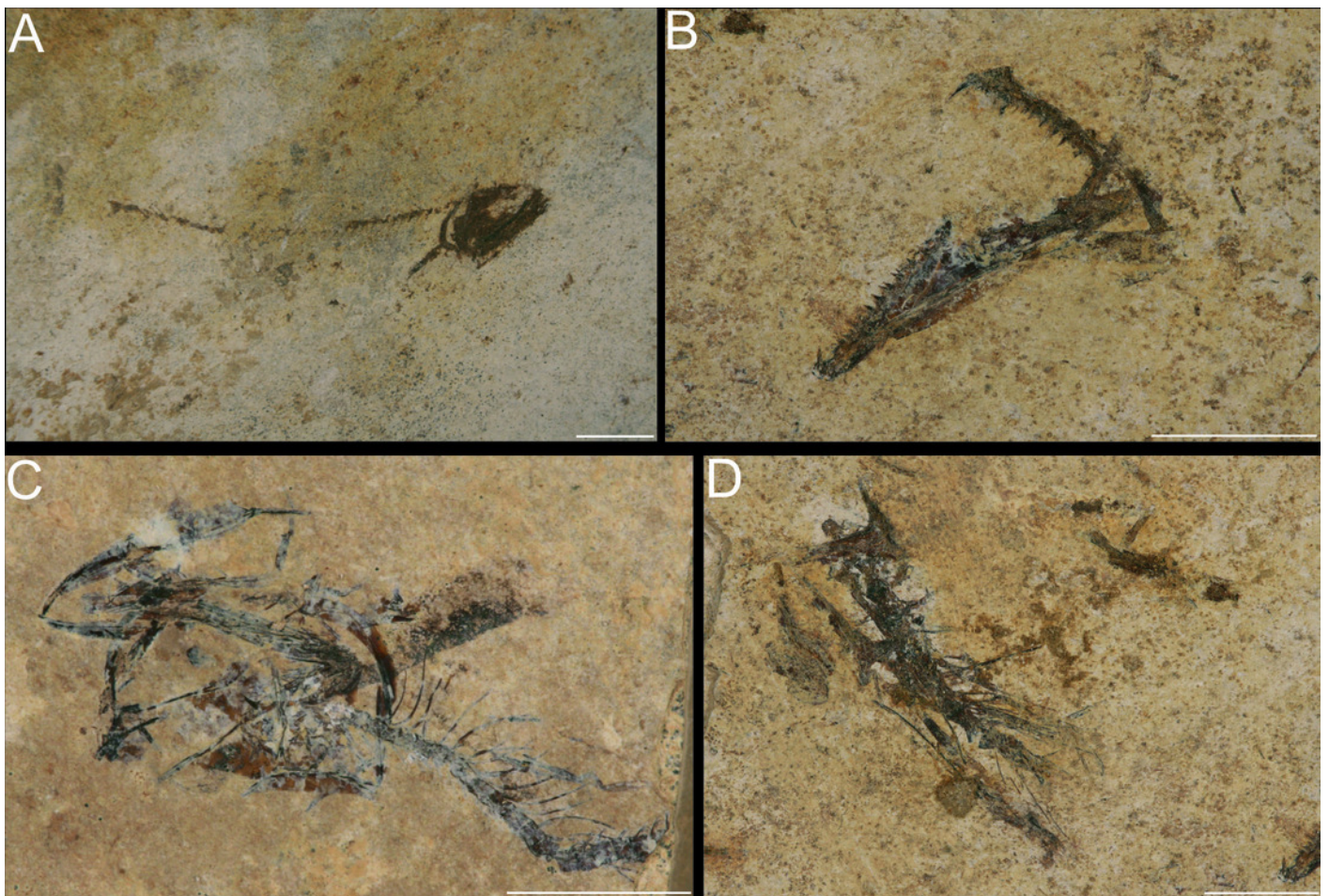


Figure 11

Examples of fossil fish from the Oligocene marine strata of the Menilite-Krosno Series (The Outer Carpathians, Poland).

(A) *Lepidopus* sp., ROU-400. (B) *Lepidopus* sp., ROU-405. (C) *Lepidopus* sp., Ma-5. (D) *Lepidopus* sp., ROU-40. (E) *Lepidopus* sp., ROU-42. (F) *Lepidopus* sp., ROL-55. (G) *Isurus* sp., ROM-ZR-100. (H) *Isurus* sp., ROM-ZR-103. (I) *Isurus* sp., ROM-ZR-107. (J) *Isurus* sp., ROM-ZR-112. (K) *Isurus* sp., ROJ-ZR-123. Scale bar equals 1 cm.

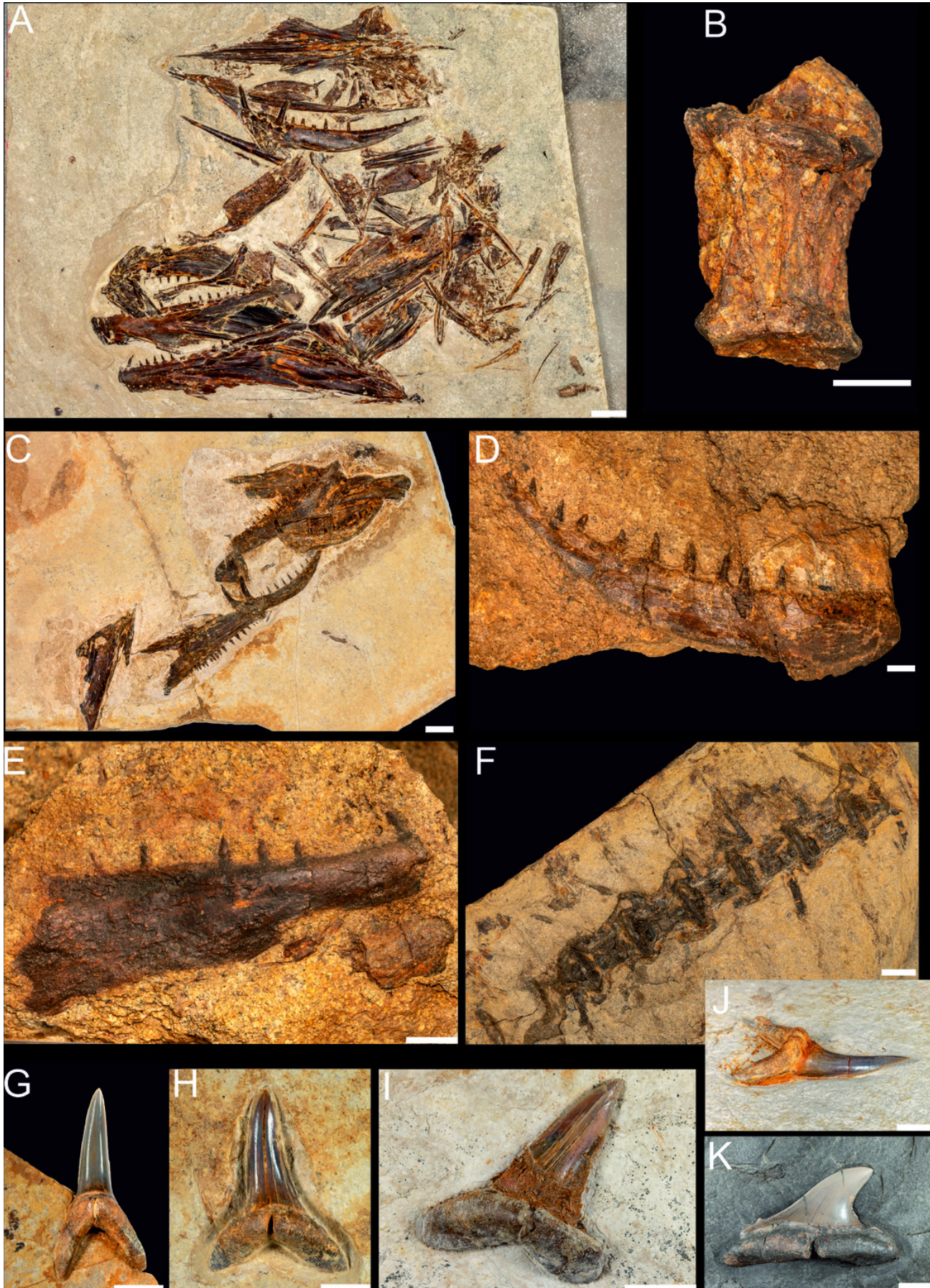


Figure 12

Examples of feathers representing unidentified taxa from the Oligocene marine strata of the Menilite-Krosno Series (The Outer Carpathians, Poland).

(A) MSMD.Av. Jam-11. (B) MSMD.Av. Jam-14. (C) MSMD.Av. S.Bir-3. (D) MSMD.Av. Jam-1. (E) MSMD.Av. J.Ros-9. (F) MSMD.Av. Jam-15. Scale bar equals 1 cm.

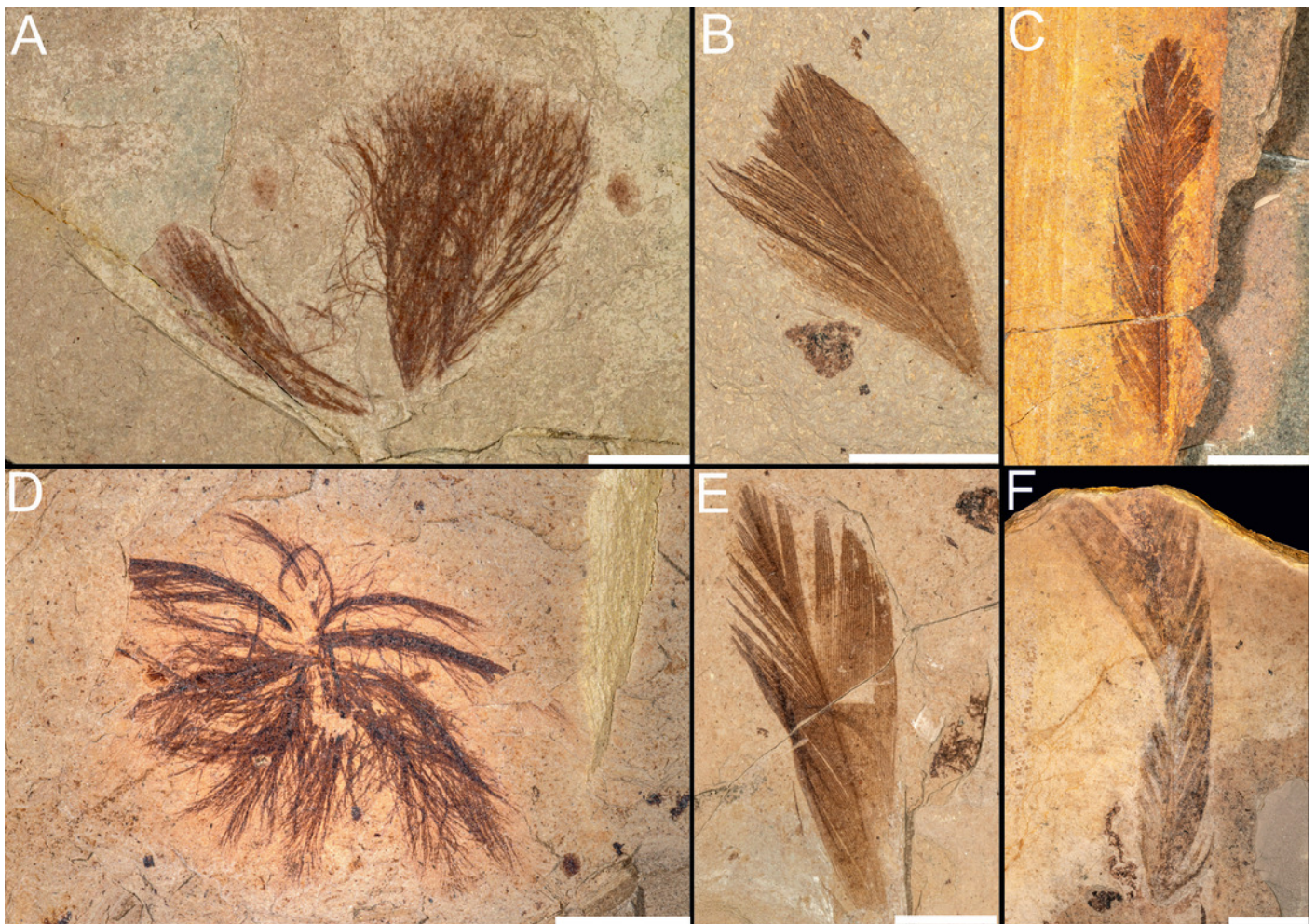


Figure 13

Some examples of vertebrate remains documented in Miocenic deposits of the Kleszczów Graben, central Poland. Acronyme number: GIUS 10-3796V.

(A) Jaw of a Lacertidae lizard. (B) Otolith of *Klingobius andjelkocae*. (C, D) Vertebrae of indetermined rodents. (E-H) Bones of indeterminate vertebrates. (I) Jaw of a rodent. (J) Tooth of Chiroptera. (K) Incisor of Castocrinae. (L-N) Talpidaeteeth. (O) Tooth of an unidentified predator. Scale bar equals 1 mm.



Table 1 (on next page)

Oligocene coprolite list.

1 **Table 1:**
 2 **Oligocene coprolite list.**
 3

Specimen	Dimensions (mm)	Shape	Age	Site
GIUS 10–3796/O/1	31x5	Sinusoidal	Oligocene - Rupelian	Menilite-Krosno Series (M-KS)-Kąkolówka I
GIUS 10–3796/O/2	23x3	Curved, Fig. 2a	Oligocene - Rupelian	M-KS-Kąkolówka I
GIUS 10–3796/O/3	22x5	Elongated	Oligocene - Rupelian	M-KS-Kąkolówka I
GIUS 10–3796/O/4	14x14	Oval	Oligocene - Rupelian	M-KS-Kąkolówka I
GIUS 10–3796/O/5	17x4	Sinusoidal	Oligocene - Rupelian	M-KS-Kąkolówka I
GIUS 10–3796/O/6	18x7	Curved	Oligocene - Rupelian	M-KS-Kąkolówka I
GIUS 10–3796/O/7	18x3	Curved, Fig.2b	Oligocene - Rupelian	M-KS-Kąkolówka I
GIUS 10–3796/O/8	25x10	Elongated	Oligocene - Rupelian	M-KS-Kąkolówka I
GIUS 10–3796/O/9	23x8	Elongated	Oligocene - Rupelian	M-KS-Kąkolówka I
GIUS 10–3796/O/10	38x9	Sinusoidal	Oligocene - Rupelian	M-KS-Kąkolówka I
GIUS 10–3796/O/11	24x19	Oval	Oligocene - Rupelian	M-KS-Kąkolówka I
GIUS 10–3796/O/12	17x9	Curved	Oligocene - Rupelian	M-KS-Kąkolówka I
GIUS 10–3796/O/13	23x6	S-shaped	Oligocene - Rupelian	M-KS-Kąkolówka I
GIUS 10–3796/O/14	29x8	Sinusoidal	Oligocene - Rupelian	M-KS-Kąkolówka I
GIUS 10–3796/O/15	35x11	Curved	Oligocene - Rupelian	M-KS-Kąkolówka I
GIUS 10–3796/O/16	38x10	Sinusoidal	Oligocene - Rupelian	M-KS-Kąkolówka I
GIUS 10–3796/O/17	41x9	Elongated	Oligocene - Rupelian	M-KS-Kąkolówka I
GIUS 10–3796/O/18	12x2	Sinusoidal	Oligocene - Rupelian	M-KS-Kąkolówka I
GIUS 10–	25x6	Curved	Oligocene -	M-KS-

3796/O/19			Rupelian	Kąkolówka I
GIUS 10– 3796/O/20	28x14	Irregular	Oligocene - Rupelian	M-KS- Kąkolówka I
GIUS 10– 3796/O/21	15x12	Oval	Oligocene - Rupelian	M-KS- Kąkolówka I
GIUS 10– 3796/O/22	17x5	Elongated	Oligocene - Rupelian	M-KS- Kąkolówka I
GIUS 10– 3796/O/23	32x2	Sinusoidal, Fig.2c	Oligocene - Rupelian	M-KS- Kąkolówka I
GIUS 10– 3796/O/24	27x5	S-shaped	Oligocene - Rupelian	M-KS- Kąkolówka I
GIUS 10– 3796/O/25	25x7	Sinusoidal	Oligocene - Rupelian	M-KS- Kąkolówka I
GIUS 10– 3796/O/26	14x4	Curved	Oligocene - Rupelian	M-KS- Kąkolówka I
GIUS 10– 3796/O/27	17x5	Elongated	Oligocene - Rupelian	M-KS- Kąkolówka I
GIUS 10– 3796/O/28	18x17	Oval	Oligocene - Rupelian	M-KS- Kąkolówka I
GIUS 10– 3796/O/29	19x6	Sinusoidal	Oligocene - Rupelian	M-KS- Kąkolówka I
GIUS 10– 3796/O/30	25x15	Irregular	Oligocene - Rupelian	M-KS- Kąkolówka I
GIUS 10– 3796/O/31	24x11	Sinusoidal	Oligocene - Rupelian	M-KS- Kąkolówka I
GIUS 10– 3796/O/32	39x9	Elongated	Oligocene - Rupelian	M-KS- Kąkolówka I
GIUS 10– 3796/O/33	26x19	Sinusoidal	Oligocene - Rupelian	M-KS- Kąkolówka I
GIUS 10– 3796/O/34	15x6	Curved	Oligocene - Rupelian	M-KS- Kąkolówka I
GIUS 10– 3796/O/35	22x7	S-shaped	Oligocene - Rupelian	M-KS- Kąkolówka I
GIUS 10– 3796/O/36	30x28	More or less regular	Oligocene - Rupelian	M-KS- Kąkolówka I
GIUS 10– 3796/O/37	14x10	More or less regular	Oligocene - Rupelian	M-KS- Kąkolówka I
GIUS 10– 3796/O/38	28x11	Sinusoidal	Oligocene - Rupelian	M-KS- Kąkolówka I
GIUS 10– 3796/O/39	34x10	Curved	Oligocene - Rupelian	M-KS- Kąkolówka I
GIUS 10– 3796/O/40	22x9	Elongated	Oligocene - Rupelian	M-KS- Kąkolówka I
GIUS 10– 3796/O/41	27x6	Sinusoidal	Oligocene - Rupelian	M-KS- Kąkolówka I
GIUS 10–	32x14	S-shaped	Oligocene -	M-KS-

3796/O/42			Rupelian	Kąkolówka I
GIUS 10– 3796/O/43	25x12	Curved	Oligocene - Rupelian	M-KS- Kąkolówka I
GIUS 10– 3796/O/44	16x5	Sinusoidal	Oligocene - Rupelian	M-KS- Kąkolówka I
GIUS 10– 3796/O/45	34x21	Irregular	Oligocene - Rupelian	M-KS- Kąkolówka I
GIUS 10– 3796/O/46	37x12	Elongated	Oligocene - Rupelian	M-KS- Kąkolówka I
GIUS 10– 3796/O/47	39x9	Sinusoidal	Oligocene - Rupelian	M-KS- Kąkolówka I
GIUS 10– 3796/O/48	14x13	Oval	Oligocene - Rupelian	M-KS- Kąkolówka I
GIUS 10– 3796/O/49	17x7	elongated	Oligocene - Rupelian	M-KS- Kąkolówka I
GIUS 10– 3796/O/50	33x9	S-shaped	Oligocene - Rupelian	M-KS- Kąkolówka I
GIUS 10– 3796/O/51	32x12	Sinusoidal	Oligocene - Rupelian	M-KS- Kąkolówka I
GIUS 10– 3796/O/52	30x14	Curved	Oligocene - Rupelian	M-KS- Kąkolówka I
GIUS 10– 3796/O/53	26x8	Elongated	Oligocene - Rupelian	M-KS- Kąkolówka I
GIUS 10– 3796/O/54	27x7	Sinusoidal	Oligocene - Rupelian	M-KS- Kąkolówka I
GIUS 10– 3796/O/55	24x21	More or less regular	Oligocene - Rupelian	M-KS- Kąkolówka I
GIUS 10– 3796/O/56	39x12	Sinusoidal	Oligocene - Rupelian	M-KS- Kąkolówka I
GIUS 10– 3796/O/57	26x8	Curved	Oligocene - Rupelian	M-KS- Kąkolówka I
GIUS 10– 3796/O/58	29x17	Irregular	Oligocene - Rupelian	M-KS- Kąkolówka I
GIUS 10– 3796/O/59	37x13	S-shaped	Oligocene - Rupelian	M-KS- Kąkolówka I
GIUS 10– 3796/O/60	38x4	Curved, Fig. 2f	Oligocene - Rupelian	M-KS- Kąkolówka I
GIUS 10– 3796/O/61	32x12	Curved	Oligocene - Rupelian	M-KS- Kąkolówka I
GIUS 10– 3796/O/62	17x16	Oval	Oligocene - Rupelian	M-KS- Kąkolówka I
GIUS 10– 3796/O/63	28x9	Sinusoidal	Oligocene - Rupelian	M-KS- Kąkolówka I
GIUS 10– 3796/O/64	39x15	Elongated	Oligocene - Rupelian	M-KS- Kąkolówka I
GIUS 10–	26x14	Sinusoidal	Oligocene -	M-KS-

3796/O/65			Rupelian	Kąkolówka I
GIUS 10– 3796/O/66	27x13	Curved	Oligocene - Rupelian	M-KS- Kąkolówka I
GIUS 10– 3796/O/67	24x10	Elongated	Oligocene - Rupelian	M-KS- Kąkolówka I
GIUS 10– 3796/O/68	23x8	Curved	Oligocene - Rupelian	M-KS- Kąkolówka I
GIUS 10– 3796/O/69	18x11	Irregular	Oligocene - Rupelian	M-KS- Kąkolówka I
GIUS 10– 3796/O/70	19x7	Sinusoidal	Oligocene - Rupelian	M-KS- Kąkolówka I
GIUS 10– 3796/O/71	28x9	S-shaped	Oligocene - Rupelian	M-KS- Kąkolówka I
GIUS 10– 3796/O/72	35x14	Sinusoidal	Oligocene - Rupelian	M-KS- Kąkolówka I
GIUS 10– 3796/O/73	37x12	Curved	Oligocene - Rupelian	M-KS- Kąkolówka I
GIUS 10– 3796/O/74	30x29	More or less regular	Oligocene - Rupelian	M-KS- Kąkolówka I
GIUS 10– 3796/O/75	50x32	Irregular	Oligocene - Rupelian	M-KS- Kąkolówka I
GIUS 10– 3796/O/76	37x15	S-shaped	Oligocene - Rupelian	M-KS- Kąkolówka I
GIUS 10– 3796/O/77	44x3	Curved, Fig. 2g	Oligocene - Rupelian	M-KS- Kąkolówka I
GIUS 10– 3796/O/78	25x4	S-shaped	Oligocene - Rupelian	M-KS- Kąkolówka I
GIUS 10– 3796/O/79	28x13	Irregular	Oligocene - Rupelian	M-KS- Kąkolówka I
GIUS 10– 3796/O/80	37x8	Sinusoidal	Oligocene - Rupelian	M-KS- Kąkolówka I
GIUS 10– 3796/O/81	28x20	More or less regular	Oligocene - Rupelian	M-KS- Kąkolówka I
GIUS 10– 3796/O/82	24x9	S-shaped	Oligocene - Rupelian	M-KS- Kąkolówka I
GIUS 10– 3796/O/83	17x5	Sinusoidal	Oligocene - Rupelian	M-KS- Kąkolówka I
GIUS 10– 3796/O/84	24x6	Sinusoidal	Oligocene - Rupelian	M-KS- Kąkolówka I
GIUS 10– 3796/O/85	29x11	Elongated	Oligocene - Rupelian	M-KS- Kąkolówka I
GIUS 10– 3796/O/86	35x8	Sinusoidal	Oligocene - Rupelian	M-KS- Kąkolówka I
GIUS 10– 3796/O/87	44x10	Irregular	Oligocene - Rupelian	M-KS- Kąkolówka I
GIUS 10–	41x15	Curved	Oligocene -	M-KS-

3796/O/88			Rupelian	Kąkolówka I
GIUS 10– 3796/O/89	19x4	Sinusoidal	Oligocene - Rupelian	M-KS- Kąkolówka I
GIUS 10– 3796/O/90	25x6	S-shaped	Oligocene - Rupelian	M-KS- Kąkolówka I
GIUS 10– 3796/O/91	38x17	Sinusoidal	Oligocene - Rupelian	M-KS- Kąkolówka I
GIUS 10– 3796/O/92	34x12	Curved	Oligocene - Rupelian	M-KS- Kąkolówka I
GIUS 10– 3796/O/93	17x5	S-shaped	Oligocene - Rupelian	M-KS- Kąkolówka I
GIUS 10– 3796/O/94	32x16	Irregular	Oligocene - Rupelian	M-KS- Kąkolówka I
GIUS 10– 3796/O/95	37x5	Curved	Oligocene - Rupelian	M-KS- Kąkolówka I
GIUS 10– 3796/O/96	21x11	Irregular	Oligocene - Rupelian	M-KS- Kąkolówka I
GIUS 10– 3796/O/97	23x9	Elongated	Oligocene - Rupelian	M-KS- Kąkolówka I
GIUS 10– 3796/O/98	15x6	Irregular, Fig. 2o	Oligocene - Rupelian	M-KS- Kąkolówka I
GIUS 10– 3796/O/99	28x8	Curved	Oligocene - Rupelian	M-KS- Kąkolówka I
GIUS 10– 3796/O/100	30x19	More or less regular	Oligocene - Rupelian	M-KS- Kąkolówka I
GIUS 10– 3796/O/101	34x10	S-shaped	Oligocene - Rupelian	M-KS- Kąkolówka I
GIUS 10– 3796/O/102	36x8	Sinusoidal	Oligocene - Rupelian	M-KS- Kąkolówka I
GIUS 10– 3796/O/103	40x13	Curved	Oligocene - Rupelian	M-KS- Kąkolówka I
GIUS 10– 3796/O/104	15x15	Oval	Oligocene - Rupelian	M-KS- Kąkolówka I
GIUS 10– 3796/O/105	17x9	Sinusoidal	Oligocene - Rupelian	M-KS- Kąkolówka I
GIUS 10– 3796/O/106	19x6	Elongated	Oligocene - Rupelian	M-KS- Kąkolówka I
GIUS 10– 3796/O/107	24x5	S-shaped, Fig. 2p	Oligocene - Rupelian	M-KS- Kąkolówka I
GIUS 10– 3796/O/108	25x4	Curved	Oligocene - Rupelian	M-KS- Kąkolówka I
GIUS 10– 3796/O/109	30x14	Irregular	Oligocene - Rupelian	M-KS- Kąkolówka I
GIUS 10– 3796/O/110	34x12	Elongated	Oligocene - Rupelian	M-KS- Kąkolówka I
GIUS 10–	18x4	S-shaped,	Oligocene -	M-KS-

3796/O/111		Fig. 2r	Rupelian	Kąkolówka I
GIUS 10– 3796/O/112	18x7	S-shaped	Oligocene - Rupelian	M-KS- Kąkolówka I
GIUS 10– 3796/O/113	15x4	Sinusoidal	Oligocene - Rupelian	M-KS- Kąkolówka I
GIUS 10– 3796/O/114	37x10	S-shaped	Oligocene - Rupelian	M-KS- Kąkolówka I
GIUS 10– 3796/O/115	20x16	Oval	Oligocene - Rupelian	M-KS- Kąkolówka I
GIUS 10– 3796/O/116	32x9	Sinusoidal	Oligocene - Rupelian	M-KS- Kąkolówka I
GIUS 10– 3796/O/117	17x11	Irregular	Oligocene - Rupelian	M-KS- Kąkolówka I
GIUS 10– 3796/O/118	33x7	Elongated	Oligocene - Rupelian	M-KS- Kąkolówka I
GIUS 10– 3796/O/119	29x8	Sinusoidal	Oligocene - Rupelian	M-KS- Kąkolówka I
GIUS 10– 3796/O/120	22x6	Curved	Oligocene - Rupelian	M-KS- Kąkolówka I
GIUS 10– 3796/O/121	41x11	Sinusoidal	Oligocene - Rupelian	M-KS- Kąkolówka I
GIUS 10– 3796/O/122	31x13	Elongated	Oligocene - Rupelian	M-KS- Kąkolówka I
GIUS 10– 3796/O/123	12x10	Oval	Oligocene - Rupelian	M-KS- Kąkolówka I
GIUS 10– 3796/O/124	25x5	Sinusoidal	Oligocene - Rupelian	M-KS- Kąkolówka I
GIUS 10– 3796/O/125	27x4	Sinusoidal	Oligocene - Rupelian	M-KS- Kąkolówka I
GIUS 10– 3796/O/126	38x9	S-shape	Oligocene - Rupelian	M-KS- Kąkolówka I
GIUS 10– 3796/O/127	35x7	Sinusoidal	Oligocene - Rupelian	M-KS- Kąkolówka I
GIUS 10– 3796/O/128	27x25	Oval	Oligocene - Rupelian	M-KS- Kąkolówka I
GIUS 10– 3796/O/129	35x10	Sinusoidal	Oligocene - Rupelian	M-KS- Kąkolówka I
GIUS 10– 3796/O/130	39x8	Elongated	Oligocene - Rupelian	M-KS- Kąkolówka I
GIUS 10– 3796/O/131	37x11	Curved	Oligocene - Rupelian	M-KS- Kąkolówka I
GIUS 10– 3796/O/132	34x6	S-shaped	Oligocene - Rupelian	M-KS- Kąkolówka I
GIUS 10– 3796/O/133	28x7	Curved	Oligocene - Rupelian	M-KS- Kąkolówka I
GIUS 10–	30x11	S-shaped	Oligocene -	M-KS-

3796/O/134			Rupelian	Kąkolówka I
GIUS 10– 3796/O/135	16x5	Curved, Fig.2s	Oligocene - Rupelian	M-KS- Kąkolówka I
GIUS 10– 3796/O/136	17x7	Sinusoidal	Oligocene - Rupelian	M-KS- Kąkolówka I
GIUS 10– 3796/O/137	20x6	Elongated	Oligocene - Rupelian	M-KS- Kąkolówka I
GIUS 10– 3796/O/138	22x13	Irregular	Oligocene - Rupelian	M-KS- Kąkolówka I
GIUS 10– 3796/O/139	32x30	Oval, Fig. 2u	Oligocene - Rupelian	M-KS- Kąkolówka I
GIUS 10– 3796/O/140	40x13	S-shaped	Oligocene - Rupelian	M-KS- Kąkolówka I
GIUS 10– 3796/O/141	37x20	Irregular	Oligocene - Rupelian	M-KS- Kąkolówka I
GIUS 10– 3796/O/142	31x15	Irregular	Oligocene - Rupelian	M-KS- Kąkolówka I
GIUS 10– 3796/O/143	33x13	Curved	Oligocene - Rupelian	M-KS- Kąkolówka I
GIUS 10– 3796/O/144	40x22	Irregular, Fig. 3c	Oligocene - Rupelian	M-KS- Kąkolówka I
GIUS 10– 3796/O/145	43x13	S-shaped	Oligocene - Rupelian	M-KS- Kąkolówka I
GIUS 10– 3796/O/146	40x10	Sinusoidal	Oligocene - Rupelian	M-KS- Kąkolówka I
GIUS 10– 3796/O/147	38x9	Curved	Oligocene - Rupelian	M-KS- Kąkolówka I
GIUS 10– 3796/O/148	23x10	Elongated	Oligocene - Rupelian	M-KS- Kąkolówka I
GIUS 10– 3796/O/149	29x6	Elongated	Oligocene - Rupelian	M-KS- Kąkolówka I
GIUS 10– 3796/O/150	17x14	Oval	Oligocene - Rupelian	M-KS- Kąkolówka I
GIUS 10– 3796/O/151	14x5	Curved	Oligocene - Rupelian	M-KS- Kąkolówka II
GIUS 10– 3796/O/152	30x8	S-shaped	Oligocene - Rupelian	M-KS- Kąkolówka II
GIUS 10– 3796/O/153	32x5	S-shaped	Oligocene - Rupelian	M-KS- Kąkolówka II
GIUS 10– 3796/O/154	14x2	Sinusoidal, Fig. 2d	Oligocene - Rupelian	M-KS- Kąkolówka II
GIUS 10–	35x8	Elongated	Oligocene -	M-KS-

3796/O/155			Rupelian	Kąkolówka II
GIUS 10–3796/O/156	22x5	Sinusoidal	Oligocene - Rupelian	M-KS-Kąkolówka II
GIUS 10–3796/O/157	32x7	S-shaped	Oligocene - Rupelian	M-KS-Kąkolówka II
GIUS 10–3796/O/158	14x3	Sinusoidal	Oligocene - Rupelian	M-KS-Kąkolówka II
GIUS 10–3796/O/159	8x6	Oval	Oligocene - Rupelian	M-KS-Kąkolówka II
GIUS 10–3796/O/160	38x6	Elongated	Oligocene - Rupelian	M-KS-Kąkolówka II
GIUS 10–3796/O/161	18x3	Sinusoidal	Oligocene - Rupelian	M-KS-Kąkolówka II
GIUS 10–3796/O/162	15x8	S-shaped	Oligocene - Rupelian	M-KS-Kąkolówka II
GIUS 10–3796/O/163	27x10	Sinusoidal	Oligocene - Rupelian	M-KS-Kąkolówka II
GIUS 10–3796/O/164	38x21	Irregular	Oligocene - Rupelian	M-KS-Kąkolówka II
GIUS 10–3796/O/165	24x9	Sinusoidal	Oligocene - Rupelian	M-KS-Kąkolówka II
GIUS 10–3796/O/166	17x8	Sinusoidal	Oligocene - Rupelian	M-KS-Kąkolówka II
GIUS 10–3796/O/167	33x6	Elongated	Oligocene - Rupelian	M-KS-Kąkolówka II
GIUS 10–3796/O/168	39x8	Curved	Oligocene - Rupelian	M-KS-Kąkolówka II
GIUS 10–3796/O/169	22x11	Irregular	Oligocene - Rupelian	M-KS-Kąkolówka II
GIUS 10–3796/O/170	41x10	Curved	Oligocene - Rupelian	M-KS-Kąkolówka

				II
GIUS 10–3796/O/171	35x13	Elongated	Oligocene - Rupelian	M-KS-Kąkolówka II
GIUS 10–3796/O/172	12x4	Sinusoidal	Oligocene - Rupelian	M-KS-Kąkolówka II
GIUS 10–3796/O/173	25x24	Oval	Oligocene - Rupelian	M-KS-Kąkolówka II
GIUS 10–3796/O/174	37x17	Elongated	Oligocene - Rupelian	M-KS-Kąkolówka II
GIUS 10–3796/O/175	15x12	Sinusoidal	Oligocene - Rupelian	M-KS-Kąkolówka II
GIUS 10–3796/O/176	19x4	Curved	Oligocene - Rupelian	M-KS-Kąkolówka II
GIUS 10–3796/O/177	19x6	S-shape	Oligocene - Rupelian	M-KS-Kąkolówka II
GIUS 10–3796/O/178	24x4	Elongated	Oligocene - Rupelian	M-KS-Kąkolówka II
GIUS 10–3796/O/179	28x7	Curved	Oligocene - Rupelian	M-KS-Kąkolówka II
GIUS 10–3796/O/180	30x8	S-shaped	Oligocene - Rupelian	M-KS-Kąkolówka II
GIUS 10–3796/O/181	11x3	Sinusoidal, Fig. 2e	Oligocene - Rupelian	M-KS-Kąkolówka II
GIUS 10–3796/O/182	33x11	Curved	Oligocene - Rupelian	M-KS-Kąkolówka II
GIUS 10–3796/O/183	19x5	Curved	Oligocene - Rupelian	M-KS-Kąkolówka II
GIUS 10–3796/O/184	20x7	Sinusoidal	Oligocene - Rupelian	M-KS-Kąkolówka II
GIUS 10–3796/O/185	15x15	Oval	Oligocene - Rupelian	M-KS-Kąkolówka II

GIUS 10– 3796/O/186	37x8	Sinusoidal	Oligocene - Rupelian	M-KS- Kąkolówka II
GIUS 10– 3796/O/187	46x15	Elongated	Oligocene - Rupelian	M-KS- Kąkolówka II
GIUS 10– 3796/O/188	34x9	Sinusoidal	Oligocene - Rupelian	M-KS- Kąkolówka II
GIUS 10– 3796/O/189	18x11	Elongated	Oligocene - Rupelian	M-KS- Kąkolówka II
GIUS 10– 3796/O/190	33x6	Curved	Oligocene - Rupelian	M-KS- Kąkolówka II
GIUS 10– 3796/O/191	29x6	Sinusoidal	Oligocene - Rupelian	M-KS- Kąkolówka II
GIUS 10– 3796/O/192	23x7	S-shaped	Oligocene - Rupelian	M-KS- Kąkolówka II
GIUS 10– 3796/O/193	42x10	Sinusoidal	Oligocene - Rupelian	M-KS- Kąkolówka II
GIUS 10– 3796/O/194	37x13	Sinusoidal	Oligocene - Rupelian	M-KS- Kąkolówka II
GIUS 10– 3796/O/195	17x4	Irregular	Oligocene - Rupelian	M-KS- Kąkolówka II
GIUS 10– 3796/O/196	28x8	Elongated	Oligocene - Rupelian	M-KS- Kąkolówka II
GIUS 10– 3796/O/197	23x4	Elongated	Oligocene - Rupelian	M-KS- Kąkolówka II
GIUS 10– 3796/O/198	35x14	Curved	Oligocene - Rupelian	M-KS- Kąkolówka II
GIUS 10– 3796/O/199	38x13	Curved	Oligocene - Rupelian	M-KS- Kąkolówka II
GIUS 10– 3796/O/200	40x17	S-shaped	Oligocene - Rupelian	M-KS- Kąkolówka II
GIUS 10–	44x10	Elongated	Oligocene -	M-KS-

3796/O/201			Rupelian	Kąkolówka II
GIUS 10–3796/O/202	17x14	Oval	Oligocene - Rupelian	M-KS-Kąkolówka II
GIUS 10–3796/O/203	35x12	S-shaped	Oligocene - Rupelian	M-KS-Kąkolówka II
GIUS 10–3796/O/204	17x6	Sinusoidal	Oligocene - Rupelian	M-KS-Kąkolówka II
GIUS 10–3796/O/205	20x7	S-shaped	Oligocene - Rupelian	M-KS-Kąkolówka II
GIUS 10–3796/O/206	18x3	S-shaped	Oligocene - Rupelian	M-KS-Kąkolówka II
GIUS 10–3796/O/207	22x9	Elongated	Oligocene - Rupelian	M-KS-Kąkolówka II
GIUS 10–3796/O/208	26x8	Sinusoidal	Oligocene - Rupelian	M-KS-Kąkolówka II
GIUS 10–3796/O/209	38x9	Curved	Oligocene - Rupelian	M-KS-Kąkolówka II
GIUS 10–3796/O/210	24x9	Sinusoidal	Oligocene - Rupelian	M-KS-Kąkolówka II
GIUS 10–3796/O/211	17x15	Oval	Oligocene - Rupelian	M-KS-Kąkolówka II
GIUS 10–3796/O/212	23x12	Irregular	Oligocene - Rupelian	M-KS-Kąkolówka II
GIUS 10–3796/O/213	31x8	Sinusoidal	Oligocene - Rupelian	M-KS-Kąkolówka II
GIUS 10–3796/O/214	35x11	Irregular	Oligocene - Rupelian	M-KS-Kąkolówka II
GIUS 10–3796/O/215	39x13	Sinusoidal	Oligocene - Rupelian	M-KS-Kąkolówka II
GIUS 10–3796/O/216	44x9	Sinusoidal	Oligocene - Rupelian	M-KS-Kąkolówka

				II
GIUS 10– 3796/O/217	12x4	Elongated	Oligocene - Rupelian	M-KS- Kąkolówka II
GIUS 10– 3796/O/218	25x7	S-shaped	Oligocene - Rupelian	M-KS- Kąkolówka II
GIUS 10– 3796/O/219	29x14	Sinusoidal	Oligocene - Rupelian	M-KS- Kąkolówka II
GIUS 10– 3796/O/220	37x13	S-shaped	Oligocene - Rupelian	M-KS- Kąkolówka II
GIUS 10– 3796/O/221	41x17	Sinusoidal	Oligocene - Rupelian	M-KS- Kąkolówka II
GIUS 10– 3796/O/222	47x11	Sinusoidal	Oligocene - Rupelian	M-KS- Kąkolówka II
GIUS 10– 3796/O/223	52x20	Sinusoidal	Oligocene - Rupelian	M-KS- Kąkolówka II
GIUS 10– 3796/O/224	31x14	Elongated	Oligocene - Rupelian	M-KS- Kąkolówka II
GIUS 10– 3796/O/225	27x26	Oval	Oligocene - Rupelian	M-KS- Kąkolówka II
GIUS 10– 3796/O/226	36x13	elongated	Oligocene - Rupelian	M-KS- Kąkolówka II
GIUS 10– 3796/O/227	38x15	S-shaped	Oligocene - Rupelian	M-KS- Kąkolówka II
GIUS 10– 3796/O/228	16x5	S-shaped	Oligocene - Rupelian	M-KS- Kąkolówka II
GIUS 10– 3796/O/229	25x8	Sinusoidal	Oligocene - Rupelian	M-KS- Kąkolówka II
GIUS 10– 3796/O/230	20x4	Elongated	Oligocene - Rupelian	M-KS- Kąkolówka II
GIUS 10– 3796/O/231	27x10	S-shaped	Oligocene - Rupelian	M-KS- Kąkolówka II

GIUS 10– 3796/O/232	26x25	Oval	Oligocene - Rupelian	M-KS- Kąkolówka II
GIUS 10– 3796/O/233	38x17	Sinusoidal	Oligocene - Rupelian	M-KS- Kąkolówka II
GIUS 10– 3796/O/234	23x11	Curved	Oligocene - Rupelian	M-KS- Kąkolówka II
GIUS 10– 3796/O/235	17x5	Elongated	Oligocene - Rupelian	M-KS- Kąkolówka II
GIUS 10– 3796/O/236	23x12	Irregular	Oligocene - Rupelian	M-KS- Kąkolówka II
GIUS 10– 3796/O/237	32x9	Sinusoidal	Oligocene - Rupelian	M-KS- Kąkolówka II
GIUS 10– 3796/O/238	35x11	Curved	Oligocene - Rupelian	M-KS- Kąkolówka II
GIUS 10– 3796/O/239	39x12	Elongated	Oligocene - Rupelian	M-KS- Kąkolówka II
GIUS 10– 3796/O/240	54x10	S-shaped	Oligocene - Rupelian	M-KS- Kąkolówka II
GIUS 10– 3796/O/241	13x4	Sinusoidal	Oligocene - Rupelian	M-KS- Kąkolówka II
GIUS 10– 3796/O/242	21x7	Curved	Oligocene - Rupelian	M-KS- Kąkolówka II
GIUS 10– 3796/O/243	29x14	Elongated	Oligocene - Rupelian	M-KS- Kąkolówka II
GIUS 10– 3796/O/244	12x3	Elongated	Oligocene - Rupelian	M-KS- Kąkolówka II
GIUS 10– 3796/O/245	36x13	Elongated	Oligocene - Rupelian	M-KS- Kąkolówka II
GIUS 10– 3796/O/246	28x11	Irregular	Oligocene - Rupelian	M-KS- Kąkolówka II
GIUS 10–	56x14	Sinusoidal	Oligocene -	M-KS-

3796/O/247			Rupelian	Kąkolówka II
GIUS 10–3796/O/248	13x11	Oval	Oligocene - Rupelian	M-KS-Kąkolówka II
GIUS 10–3796/O/249	22x7	Curved	Oligocene - Rupelian	M-KS-Kąkolówka II
GIUS 10–3796/O/250	29x16	Curved	Oligocene - Rupelian	M-KS-Kąkolówka II
GIUS 10–3796/O/251	17x4	Elongated, Fig. 2h	Oligocene - Rupelian	M-KS-Wola Czudecka
GIUS 10–3796/O/252	39x15	elongated	Oligocene - Rupelian	M-KS-Wola Czudecka
GIUS 10–3796/O/253	13x3	Elongated, Fig. 2i	Oligocene - Rupelian	M-KS-Wola Czudecka
GIUS 10–3796/O/254	19x4	S-shaped	Oligocene - Rupelian	M-KS-Wola Czudecka
GIUS 10–3796/O/255	28x10	Sinusoidal	Oligocene - Rupelian	M-KS-Wola Czudecka
GIUS 10–3796/O/256	33x15	Irregular	Oligocene - Rupelian	M-KS-Wola Czudecka
GIUS 10–3796/O/257	37x8	S-shaped	Oligocene - Rupelian	M-KS-Wola Czudecka
GIUS 10–3796/O/258	39x11	Curved	Oligocene - Rupelian	M-KS-Wola Czudecka
GIUS 10–3796/O/259	10x4	Elongated, Fig. 2j	Oligocene - Rupelian	M-KS-Wola Czudecka
GIUS 10–3796/O/260	39x9	Elongated	Oligocene - Rupelian	M-KS-Wola Czudecka
GIUS 10–3796/O/261	36x13	Sinusoidal	Oligocene - Rupelian	M-KS-Wola Czudecka
GIUS 10–3796/O/262	24x24	Oval	Oligocene - Rupelian	M-KS-Wola Czudecka
GIUS 10–3796/O/263	15x7	Curved	Oligocene - Rupelian	M-KS-Wola Czudecka
GIUS 10–3796/O/264	26x5	Sinusoidal	Oligocene - Rupelian	M-KS-Wola Czudecka
GIUS 10–3796/O/265	33x14	Irregular	Oligocene - Rupelian	M-KS-Wola Czudecka
GIUS 10–3796/O/266	14x4	Curved	Oligocene - Rupelian	M-KS-Wola Czudecka
GIUS 10–3796/O/267	36x13	Sinusoidal	Oligocene - Rupelian	M-KS-Wola Czudecka
GIUS 10–	38x11	Elongated	Oligocene -	M-KS-Wola

3796/O/268			Rupelian	Czudecka
GIUS 10– 3796/O/269	50x22	S-shaped	Oligocene - Rupelian	M-KS-Wola Czudecka
GIUS 10– 3796/O/270	12x13	Sinusoidal	Oligocene - Rupelian	M-KS-Wola Czudecka
GIUS 10– 3796/O/271	28x7	Elongated	Oligocene - Rupelian	M-KS-Wola Czudecka
GIUS 10– 3796/O/272	35x14	Curved	Oligocene - Rupelian	M-KS-Wola Czudecka
GIUS 10– 3796/O/273	21x18	Oval	Oligocene - Rupelian	M-KS-Wola Czudecka
GIUS 10– 3796/O/274	20x4	Elongated, Fig. 2k	Oligocene - Rupelian	M-KS-Wola Czudecka
GIUS 10– 3796/O/275	42x16	Elongated	Oligocene - Rupelian	M-KS-Wola Czudecka
GIUS 10– 3796/O/276	38x5	Sinusoidal	Oligocene - Rupelian	M-KS-Wola Czudecka
GIUS 10– 3796/O/277	39x9	S-shaped	Oligocene - Rupelian	M-KS-Wola Czudecka
GIUS 10– 3796/O/278	41x13	Sinusoidal	Oligocene - Rupelian	M-KS- Futoma
GIUS 10– 3796/O/279	11x9	Oval, Fig. 2l	Oligocene - Rupelian	M-KS- Futoma
GIUS 10– 3796/O/280	11x4	Elongated	Oligocene - Rupelian	M-KS- Futoma
GIUS 10– 3796/O/281	19x6	S-shaped	Oligocene - Rupelian	M-KS- Futoma
GIUS 10– 3796/O/282	9x4	Irregular, Fig. 2m	Oligocene - Rupelian	M-KS- Futoma
GIUS 10– 3796/O/283	33x9	Sinusoidal	Oligocene - Rupelian	M-KS- Futoma
GIUS 10– 3796/O/284	35x11	Curved	Oligocene - Rupelian	M-KS- Futoma
GIUS 10– 3796/O/285	32x13	Elongated	Oligocene - Rupelian	M-KS- Wujskie
GIUS 10– 3796/O/286	20x7	Sinusoidal	Oligocene - Rupelian	M-KS- Wujskie
GIUS 10– 3796/O/287	26x5	Sinusoidal	Oligocene - Rupelian	M-KS- Wujskie
GIUS 10– 3796/O/288	11x3	Elongated	Oligocene - Rupelian	M-KS- Wujskie
GIUS 10– 3796/O/289	19x4	Elongated	Oligocene - Rupelian	M-KS- Rudawka Rymanowsk a
GIUS 10–	45x15	Sinusoidal	Oligocene -	M-KS-

3796/O/290			Rupelian	Rudawska Rymanowsk a
GIUS 10– 3796/O/291	28x15	Sinusoidal	Oligocene - Rupelian	M-KS- Rudawka Rymanowsk a
GIUS 10– 3796/O/292	14x11	Oval	Oligocene - Rupelian	M-KS-Jamna Dolna
GIUS 10– 3796/O/293	57x10	Curved	Oligocene - Rupelian	M-KS-Jamna Dolna
GIUS 10– 3796/O/294	10x4	Elongated, Fig. 2t	Oligocene - Rupelian	M-KS-Jamna Dolna
GIUS 10– 3796/O/295	19x13	Irregular	Oligocene - Rupelian	M-KS-Jamna Dolna
GIUS 10– 3796/O/296	22x7	Elongated	Oligocene - Rupelian	M-KS-Jamna Dolna
GIUS 10– 3796/O/297	9x7	Oval, Fig. 3a	Oligocene - Rupelian	M-KS- Równe
GIUS 10– 3796/O/298	13x13	Oval	Oligocene - Rupelian	M-KS- Równe
GIUS 10– 3796/O/299	54x6	Sinusoidal, Fig.3b	Oligocene - Rupelian	M-KS- Jasienica Rosielna
GIUS 10– 3796/O/300	20x4	Curved	Oligocene - Rupelian	M-KS- Jasienica Rosielna

4

5

Table 2 (on next page)

Miocene coprolite list.

1 **Table 2:**
 2 **Miocene coprolite list.**
 3

Specimen	Dimensions (mm)	Shape	Age	Site
GIUS 10–3796/M/1	36x28	Oval	Miocene - Langhian	Kleszczów Graben area-Belchatów
GIUS 10–3796/M/2	25x15	Irregular, Fig. 3l	Miocene - Langhian	Kleszczów Graben area-Belchatów
GIUS 10–3796/M/3	19x17	Oval	Miocene - Langhian	Kleszczów Graben area-Belchatów
GIUS 10–3796/M/4	21x17	Oval	Miocene - Langhian	Kleszczów Graben area-Belchatów
GIUS 10–3796/M/5	27x8	Curved	Miocene - Langhian	Kleszczów Graben area-Belchatów
GIUS 10–3796/M/6	20x10	Elongated, Fig. 3m	Miocene - Langhian	Kleszczów Graben area-Belchatów
GIUS 10–3796/M/6(1)	18x8	Elongated	Miocene - Langhian	Kleszczów Graben area-Belchatów
GIUS 10–3796/M/6(2)	16x10	Elongated	Miocene - Langhian	Kleszczów Graben area-Belchatów
GIUS 10–3796/M/6(3)	19x11	Elongated	Miocene - Langhian	Kleszczów Graben area-Belchatów
GIUS 10–3796/M/6(4)	15x8	Elongated	Miocene - Langhian	Kleszczów Graben area-Belchatów
GIUS 10–3796/M/6(5)	19x12	Elongated	Miocene - Langhian	Kleszczów Graben area-Belchatów
GIUS 10–3796/M/7	27x25	Oval	Miocene - Langhian	Kleszczów Graben area-Belchatów
GIUS 10–3796/M/8	37x13	Elongated	Miocene - Langhian	Kleszczów Graben area-Belchatów
GIUS 10–	47x18	Irregular	Miocene -	Kleszczów

3796/M/9			Langhian	Graben area- Bełchatów
GIUS 10– 3796/M/10	31x30	Oval	Miocene - Langhian	Kleszczów Graben area- Bełchatów
GIUS 10– 3796/M/11	25x20	Oval, Fig. 3n	Miocene - Langhian	Kleszczów Graben area- Bełchatów
GIUS 10– 3796/M/12	16x5	Sinusoidal	Miocene - Langhian	Kleszczów Graben area- Bełchatów
GIUS 10– 3796/M/13	20x8	Elongated, Fig. 3e	Miocene - Langhian	Gołuchów quarry
GIUS 10– 3796/M/14	40x14	S-shaped	Miocene - Burdigalian	Turów area
GIUS 10– 3796/M/15	61x24	Curved	Miocene - Burdigalian	Turów area
GIUS 10– 3796/M/16	50x20	Elongated, Fig. 3g	Miocene - Burdigalian	Turów area
GIUS 10– 3796/M/17	34x24	Oval	Miocene - Burdigalian	Turów area
GIUS 10– 3796/M/18	41x13	S-shaped	Miocene - Burdigalian	Turów area
GIUS 10– 3796/M/19	55x17	Curved, Fig. 3h	Miocene - Burdigalian	Turów area
GIUS 10– 3796/M/20	36x18	Elongated	Miocene - Burdigalian	Turów area
GIUS 10– 3796/M/21	40x14	Sinusoidal	Miocene - Burdigalian	Turów area
GIUS 10– 3796/M/22	31x10	S-shaped	Miocene - Burdigalian	Turów area
GIUS 10– 3796/M/23	62x31	Irregular, Fig. 3i	Miocene - Burdigalian	Turów area
GIUS 10– 3796/M/24	54x23	Sinusoidal	Miocene - Burdigalian	Turów area
GIUS 10– 3796/M/25	36x16	Sinusoidal	Miocene - Burdigalian	Turów area
GIUS 10– 3796/M/26	30x30	Oval	Miocene - Burdigalian	Turów area
GIUS 10– 3796/M/27	48x19	Elongated	Miocene - Burdigalian	Turów area
GIUS 10– 3796/M/28	78x20	Curved, Fig.3j	Miocene - Burdigalian	Turów area
GIUS 10– 3796/M/29	73x25	Elongated	Miocene - Burdigalian	Turów area
GIUS 10–	66x27	S-shaped,	Miocene -	Turów area

3796/M/20		Fig. 3k	Burdigalian	
GIUS 10– 3796/M/31	41x13	Curved	Miocene - Burdigalian	Turów area
GIUS 10– 3796/M/32	33*14	Elongated, Fig. 3f	Miocene - Serravalian	Roztocze area- Żelebsko
GIUS 10– 3796/M/33	23x5	Elongated, Fig. 3d	Miocene - Burdigalian	M-KS- Temeszów
GIUS 10– 3796/M/34	30x10	Elongated	Miocene - Burdigalian	M-KS- Brzuska

4

Table 3 (on next page)

Oligocene localities with coprolites and their morphologies.

- 1 **Table 3:**
 2 **Oligocene localities with coprolites and their morphologies.**
 3

Locality	SHAPE						Summary
	Sinusoidal	Elongated	Oval	More or less regular	S-shaped	Curved	
M-KS-Kąkolówka I	40	23	18	17	22	30	150
M-KS-Kąkolówka II	34	21	8	7	17	13	100
M-KS-Wola Czudecka	6	9	2	1	4	5	27
M-KS-Futoma	2	1	1	1	1	1	7
M-KS-Jamna Dolna	-	2	1	1	-	1	5
M-KS-Rudawka Rymanowska	2	1	-	-	-	-	3
M-KS-Równe	-	-	2	-	-	-	2
M-KS-Wujskie	2	2	-	-	-	-	4
M-KS-Jasienica Rosielna	1	-	-	-	-	1	2

4

Table 4 (on next page)

Miocene localities with coprolites and their morphologies.

- 1 **Table 4:**
 2 **Miocene localities with coprolites and their morphologies.**
 3

Locality	SHAPE						Summary
	Sinusoidal	Elongated	Oval	More or less regular	S-shaped	Curved	
Kleszczów Graben area	5	9	2	1	-	1	17
Turów area	3	4	2	1	4	4	18
Gołuchów quarry	-	1	-	-	-	-	1
Roztocze area-Żelebsko							1
M-KS-Temeszów	-	1	-	-	-	-	1
M-KS-Brzuska	-	1	-	-	-	-	1

4